

Cross-frequency coupling and sleep-dependent declarative memory consolidation: sleep states  
as opponent processes

Jordan O'Byrne

A Thesis  
in  
The Department  
of  
Exercise Science

Presented in Partial Fulfillment of Requirements  
for the Degree of Master of Science (Neuroscience) at  
Concordia University  
Montreal, Quebec, Canada

December 2016

© Jordan O'Byrne, 2016

CONCORDIA UNIVERSITY  
School of Graduate Studies

This is to certify that the thesis prepared

By: \_\_\_\_\_

Entitled: \_\_\_\_\_

and submitted in partial fulfillment of the requirements for the degree of

\_\_\_\_\_

complies with the regulations of the University and meets the accepted standards with respect to originality and quality.

Signed by the final examining committee:

Dr. Nancy St-Onge \_\_\_\_\_ Chair

Dr. Richard Courtemanche \_\_\_\_\_ Examiner

Dr. Sylvain Baillet \_\_\_\_\_ Dr. Sylvain Williams Examiner

Dr. Thien Thanh Dang-Vu \_\_\_\_\_ Supervisor

Approved by \_\_\_\_\_  
Chair of Department or Graduate Program Director

\_\_\_\_\_  
Dean of Faculty

Date \_\_\_\_\_

## ABSTRACT

Cross-frequency coupling and sleep-dependent declarative memory consolidation: sleep states as opponent processes

Jordan O'Byrne

Cross-frequency coupling (CFC) binds neuronal oscillations in sleep and wake, but the mnemonic function of these interactions remains unclear. We recorded scalp electroencephalography from 10 human participants while they slept following a declarative word pair learning task or a non-learning control task. In non rapid-eye-movement sleep (NREMS), delta-sigma phase-amplitude coupling (PAC) was marginally increased in central regions after learning, and its learning-related change in frontal regions was strongly predictive of recall performance the next morning. We observed opposite effects for CFC in rapid-eye-movement sleep (REMS). Delta- and theta-gamma PAC were still significantly increased after learning at fronto-central locations, but the frontal increase was negatively correlated with subsequent recall performance. Importantly, characteristics of the coupled oscillations (delta/slow waves and sigma/spindles in NREMS, and delta, theta and gamma in REMS) showed no learning-related effect. Only their synchronization was mnemonically significant. We propose that NREMS and REMS are opponent processes in their effect on declarative memory consolidation. Whereas NREMS integrates new memories to the knowledge network and stabilizes learned associations through temporally ordered thalamo-cortico-hippocampal reactivations, REMS brings out weak links and encodes them through hippocampo-cortical delta- and theta-gamma PAC, thus weakening the accuracy of waking memories. This interplay is analogous to the trade-off between exploration and exploitation in decision-making research and artificial intelligence.

Keywords: cross-frequency coupling, phase-amplitude coupling, sleep, memory consolidation

## **Acknowledgements**

This work was completed with scholarship support from the Canadian Institutes of Health Research (CIHR), from the Fonds de Recherche du Québec – Santé (FRQ-S) and financial support from Dr. Dang-Vu. The research project was funded by the Natural Sciences and Engineering Research Council (NSERC). I would like to gratefully acknowledge the contributions of these individuals in data collection: Soufiane Boucetta, Ali Salimi, Benjamin Hatch, Dylan Smith, Corina Moraru, Elisabeth Houle, Shira Azoulay, Cynthia Malu, Alex Nguyen, Victoria Zhang, Oupamdeep Malhi, Lindsay Reed, Aurée Arcelin, Vivane Guignard, Sylviane Guignard, Arshi Kaffash, Nabeel Ali, Victoria You, Antony Rossi, Julia Alessi, Vanessa Del Vecchio, Jocelyn Jia, Elise Arsenault, Melissa Berman Rosa, Vanessa Discepola, Kirsten Packwood, Melissa Veenstra, Lena Dakin, Stephanie McKenzie, Marilia Bedendi, Neressa Noel, Molly Brisebois and Kerstin Wenzel. Thanks to Giovanni Piantoni and Adriano Tort for sharing their code. Thanks to Zarish Abbas for helpful discussions. Special thanks to Oren Weiner, Claire André, Eden Debellemanière and Julia Giraud for their help in recruitment, data collection, scoring, and for their support. Thanks to my committee, Dr Courtemanche, Dr Williams and Dr Baillet, and to my supervisor, Dr Dang-Vu, for their input and support.

## **Contribution of Authors**

JOB devised the study design in consultation with Dr. Dang-Vu. JOB completed the majority of the recruitment, data collection and half of the sleep staging, with help from the Dang-Vu laboratory. JOB completed all analyses, reporting and writing.

## Table of Contents

Introduction.....	1
Methods.....	3
<i>Participants</i> .....	3
<i>Polysomnography</i> .....	4
<i>Tasks</i> .....	5
<i>Data analysis</i> .....	6
<i>Discrete slow wave detection</i> .....	7
<i>Discrete spindle detection</i> .....	7
<i>Discrete detection-based cross-frequency coupling</i> .....	8
<i>Phase-amplitude coupling</i> .....	8
<i>Phase analysis</i> .....	10
<i>Comodulogram</i> .....	10
<i>Statistics</i> .....	11
Results.....	13
<i>Participant sample</i> .....	13
<i>Learning task</i> .....	13
<i>Power spectra</i> .....	14
<i>Discrete oscillatory events</i> .....	14
<i>Phase-amplitude coupling with a priori bands</i> .....	16
<i>Phase analysis</i> .....	17
<i>Comodulogram</i> .....	18
Discussion.....	19
<i>NREMS CFC and learning</i> .....	20
<i>REMS CFC and learning</i> .....	22
<i>Differences in CFC by stage</i> .....	23
<i>Significance of sleep CFC for learning</i> .....	23
<i>Limitations</i> .....	28
<i>Next steps</i> .....	30
<i>Concluding remarks</i> .....	30
References.....	32
Tables.....	43
Figures.....	58

## Introduction

In the mammalian brain, electrical activity is segregated in space and time. The mechanisms of spatial segregation are well described, mainly in the form of synaptic connections and modular brain organization. Only recently has temporal segregation in the brain received comparable attention, in the study of neuronal oscillations (Varela et al., 2001; Buzsáki, 2006). The brain resounds with these electric field fluctuations, at frequencies spanning five orders of magnitude (Buzsáki and Draguhn, 2004). Far from independent, they are embedded in one another (Soltesz and Deschênes, 1993; Jensen and Colgin, 2007; Canolty and Knight, 2010; Engel et al., 2013), like nested for-loops in a computer program. Whether this rhythmic multiplexing is functional, or merely incidental, is the subject of intense research.

Sleep, perhaps better than any behaviour, displays the complex hierarchy of neuronal oscillations (Steriade et al., 1993; Steriade, 2006). In non-rapid-eye-movement (NREMS), the depolarizing up-state of slow waves (0.25-4 Hz; SW) from the neocortex encloses thalamocortical sleep spindles (10-16 Hz) (Contreras and Steriade, 1995), which themselves nest hippocampal sharp-wave ripples (SPW-R) within their troughs (Siapas and Wilson, 1998; Sirota et al., 2003). SPW-Rs in turn group the pairwise synchronous firing of single neurons in the hippocampal CA1 region (Wilson and McNaughton, 1994), joining the overarching multi-second to the elementary millisecond scale. Likewise, neocortical gamma (> 30 Hz) power in NREMS is biased by the phase of concurrent spindle (Peyrache et al., 2011; Ayoub et al., 2012; Takeuchi et al., 2016), slow (Hasenstaub et al., 2005; Isomura et al., 2006) and infraslow (> 10 s) (Leopold et al., 2003) oscillations. Early work describing SW-spindle cross-frequency coupling (CFC) in animal NREMS has now been replicated in human scalp (Mölle et al., 2002; Piantoni et al., 2013; Klinzing et al., 2016), subdural (Clemens et al., 2007) and intracranial (Staresina et al., 2015) electroencephalography (EEG). In rapid-eye-movement sleep (REMS), animal studies have shown that the phase of the hippocampal theta (4-8 Hz) rhythm, a reliable high-power rhythm also observed in waking locomotion, modulates the amplitude of neocortical gamma (Montgomery et al., 2008; Scheffer-Teixeira et al., 2011; Scheffzük et al., 2011). This type of CFC is known as phase-amplitude coupling (PAC). Similar coupling was observed in human REMS (Clemens et al., 2009; Amiri et al., 2016), albeit at a delta (1-4 Hz) rather than a theta phase frequency. Still, these coupling dynamics may be homologous (Bódizs et al., 2001; Jacobs, 2014), considering that the ratio of oscillatory frequency to brain size seems evolutionarily preserved (Buzsáki and Mizuseki, 2013).

The precise and well-preserved complexity of temporal organization in the brain, particularly during sleep, suggests a functional importance. Much recent work has made the case for an active role of sleep-dependent oscillations in memory consolidation (reviewed in Rasch and Born, 2013). In a landmark series of experiments, transcranial induction of ersatz SWs in the human prefrontal cortex during early sleep resulted in an improvement in next-day word pair recall, as well as an increase in endogenous SWs and spindles (Marshall et al., 2006), while 5-Hz rhythm induction reduced SWs, spindles and subsequent word pair recall (Marshall et al., 2011). In a later study by the same group, word pair recall enhancement was achieved instead by boosting SW amplitude with in-phase auditory stimulation (Ngo et al., 2013). As for spindles, a number of correlative behavioural studies in humans (Gais et al., 2002; Schabus et al., 2004; Cox et al., 2012) are complemented by a human pharmacological experiment (Mednick et al., 2013) in support of their role in declarative memory consolidation. The role of hippocampal SPW-Rs in memory consolidation (Buzsáki, 1989) has received support from correlative behavioural studies (Axmacher et al., 2008; Eschenko et al., 2008) and a loss-of-function experiment in rats (Girardeau et al., 2009). The contribution of REMS-specific rhythms to memory consolidation is debated (Siegel, 2001; Vertes, 2004; Walker and Stickgold, 2004). A recent optogenetic experiment in rats supports an active involvement of hippocampal theta, showing that its selective abolishment during REMS led to a decrement in contextual memory post-sleep (Boyce et al., 2016).

Sleep-dependent oscillations, then, appear to be more than an epiphenomenon (Nunez, 1981). But what of their interactions? It remains unclear whether temporal organization remains functional at higher, rhythm-multiplexing scales. There is a wealth of research linking waking CFC, especially theta-gamma PAC, to learning and memory in rats (Shirvalkar et al., 2009; Tort et al., 2009) and humans (Jensen, 2006; Osipova et al., 2006; Sauseng et al., 2009; Axmacher et al., 2010; Kaplan et al., 2014; Lega et al., 2014; Sweeney-Reed et al., 2014), but despite the recent proliferation of mnemonic models involving CFC in sleep (Diekelmann and Born, 2010; Lewis and Durrant, 2011; Rasch and Born, 2013; Staresina et al., 2015), little experimental attention has been devoted to the specific association between sleep CFC and memory consolidation. A study in humans demonstrated that spindle density during SW-rich deep sleep better predicted overnight declarative memory retention than during SW-sparse light sleep, indicating that these oscillations may functionally interact (Cox et al., 2012); however, precise CFC was not examined. To date, three studies have specifically linked sleep CFC with memory consolidation, all of them in NREMS. Two studies by Mölle and colleagues (2009; 2011) found that learning enhanced the clustering of spindles during SW up-states, while Niknazar et al.

(2015) observed that coordination of spindle peaks during the SW up-state transition predicted better declarative memory performance after an early morning nap. To our knowledge, REMS CFC has not been examined in relation to memory consolidation. A comprehensive investigation is warranted, examining the interactive effects from declarative learning to NREMS and REMS CFC, to next-day recall.

In this study, we recorded the scalp EEG of 10 human participants as they slept following either a declarative word pair learning task or a non-learning control task. We first asked whether the type of task altered CFC measures during sleep, and next, whether these measures predicted recall performance the next morning. We found differential effects of the learning task on CFC among stages and frequency bands, detected at the frontal and central midline. In REMS, beta/gamma modulation by the theta rhythm was markedly enhanced after the learning task, as was delta-gamma PAC, albeit to a lesser extent. Conversely, NREMS theta-gamma PAC was reduced with learning. Delta-sigma PAC in early NREMS was at once marginally increased by learning and strongly predictive of better recall in the morning test, whereas in REMS, theta-gamma and delta-gamma PAC increases were associated with poor morning recall. Together, these findings indicate that declarative learning triggers multiplexing processes in the sleeping brain which seem conducive to recall in NREMS, and detrimental to it in REMS.

## **Methods**

Participants slept three nights in the laboratory: one first night of polysomnographic (PSG) sleep screening and environmental adaptation, and two PSG/EEG experimental nights. Each night was scheduled one week apart. Experimental nights involved a learning task or a non-learning control task, and their order was counterbalanced between participants. Both tasks consisted of a pre-sleep and a post-sleep component, scheduled such as to provide a 30-minute buffer with participants' usual bedtime and wake time (Fig. 1).

### *Participants*

Ten young, healthy volunteers (5 females, 5 males, mean age  $\pm$  SD: 23.7  $\pm$  3.2 years) took part in the study. Volunteers were recruited through an advertisement in the "students and part-time work" section of an online classified service. Respondents to the advertisement were first taken through a short telephone screening, followed by online questionnaires and an in-person semi-structured interview. The telephone and in-person screening ruled out the following exclusion criteria: acute and chronic medical conditions, including sleep (e.g. insomnia, sleep apnea) and

psychiatric disorders (e.g. depression); current use of psychotropic medication (other than contraceptives) or recreational drugs; excessive alcohol or tobacco use; recent (<2 months) travel further than one time zone; current or recent (<1 year) night shift work; and pregnancy. In addition, respondents had to meet these inclusion criteria: age between 18 and 30, inclusively; native French literacy; and right-handedness. French literacy was required for the French-language paired associates task. Right-handedness was required to homogenize the lateralization of brain activity. The online screening questionnaires included the Centre for Epidemiological Studies – Depression screening (CES-D) for depression screening (cutoff at CES-D > 15) and the morningness-eveningness questionnaire (MEQ) to rule out excessively early (MEQ > 70) or late (MEQ < 30) sleep schedules. Admitted participants completed a battery of additional sleep and psychological questionnaires to confirm their eligibility. Sleep disturbances were measured using the Pittsburgh sleep quality index (PSQI) the Epworth sleepiness scale (ESS) and the insomnia severity index (ISI). Psychological questionnaires consisted of Beck's depression inventory (BDI) and the Beck Anxiety Inventory (BAI). The Edinburgh Handedness Inventory (EHI) was also administered to confirm right-handedness (see Table 1). P The participants were fitted with actigraphy watches (Respironics Actiwatch 2) for the entire 2-week period of the study, to monitor their sleep and ensure they were not sleep deprived on experimental nights. Participants who did not maintain regular sleep schedules during the study period were excluded. Prior to participation in the study, volunteers signed an informed consent form, which was approved by the Concordia University Human Research Ethics Committee and the Comité d'éthique de la recherche de l'IUGM.

### *Polysomnography*

Eligible participants underwent a first overnight evaluation of their sleep at the IUGM sleep laboratory. The full PSG array consisted of 12-channel EEG placed according to the 10-20 system and referenced to Pz, as well as electrooculography (EOG), submental electromyography (EMG), electrocardiography (ECG), leg EMG, nasal-oral thermocouple airflow, nasal pressure airflow, thoracic and abdominal pressure belts, transcutaneous finger pulse oximetry and a pharyngeal microphone. PSG was recorded with the Somnoscreen plus PSG system and digitally stored using the Domino analysis software (Somnomedics, Randersacker, Germany). The first PSG night provided a final screening for sleep disorders (insomnia, sleep apnea, narcolepsy, hypersomnia, restless legs syndrome). A trained sleep technician scored the recordings for sleep and breathing anomalies (sleep apnea syndrome defined by an apnea-hypopnea index > 5/h), and eligible participants were definitively admitted

to the study. Admitted participants then underwent two more PSG nights, the learning night and control night, scheduled 7 days apart. For these recordings, breathing measures were substituted for a full EEG montage, with 18 EEG channels (Fz, F3, F4, F7, F8, Cz, C3, C4, T3, T4, P3, P4, T5, T6, O1, O2, M1, M2, Pz reference, Fpz ground), electrooculography, electrocardiography and chin electromyography. Participants were asked to keep regular sleep-wake schedules prior to the study (verified by actigraphy) and to refrain from consuming caffeinated beverages after noon on recording days, and were required to have had a meal before arriving at the laboratory. They went to bed at their habitual bedtime (no later than 12:30 AM) and slept until they awoke spontaneously (no later than 9 AM). In the morning, participants were offered a light, caffeine-free breakfast 10 minutes after awakening.

### *Tasks*

Two hours prior to their bedtime each night, participants performed one of two cognitive tasks, in an order counterbalanced between participants (Fig. 1). The learning task was a variant of the paired associates task (Plihal and Born, 1997), performed on a laptop computer in a private room (Fig. 1). All instructions were provided onscreen, in French. Participants were asked to memorize 120 word-pair associations, presented twice onscreen in a scrambled order. The first presentation of each word pair was 5 s long, with a 5-s rest and 3-s readiness cross, and the second presentation was 3 s long, with a 3-s rest and 3-s readiness cross, for a total learning time of 45 min. In order to homogenize memorization strategies, participants were instructed to use the rest period to form a mental image incorporating both words. For instance, if the words were *tasse* (cup) and *sable* (sand), one could imagine a cup filled with sand. It was also specified in the instructions that participants would be tested on recall of the second word (target) upon presentation of the first (cue). Words were randomly selected from an open online French word frequency table (New et al., 2001). Only singular-form nouns five to nine letters long with frequency greater than five per million were chosen. Nouns were further selected for concreteness and low emotional salience. Nouns were paired randomly, and resultant pairs that were semantically related were further scrambled, so that all word pairs were semantically unrelated. After both presentation phases, participants performed cued recall. In this phase, a research assistant was present in the room and participants were presented with the cues onscreen, in a scrambled order. They were asked to verbally recall the associated target. Unlimited time was allowed for recall of each word, and participants proceeded to the next cue by pressing a button. The research assistant scored the answers but provided no feedback to the participant. Each of the pre-sleep phases was punctuated by 2-min breaks. In the morning,

~30 min after awakening, participants repeated the test phase with the cues in a scrambled order. The non-learning task was based on Gais et al. (2002) and was designed to resemble the learning task in its duration, structure, visual appearance and difficulty, but without the declarative learning component (Fig. 1). Participants were presented with pairs of nonsense strings of letters (e.g. BSAVAEC), and were asked to count and verbally state the number of letters containing curved lines (e.g. B, C and S, but not A, E and V). The presentation, rest and readiness cross durations were identical to the learning task, with one long phase and two short phases (the second short phase replacing the test phase). In the morning, participants completed a fourth phase ~30 min after awakening. Nonsense words were randomly generated by scrambling the letters in the concatenated list of learning task words, and sectioning it into 240 five- to nine-letter strings. New lists were generated for each of the four phases, to avoid implicit learning. To better mimic the learning task, a research assistant was present in the room for the third and fourth phases, recording answers without feedback. EEG was recorded throughout the tasks, and each pre/post component was bounded by 5-minute quiet wakefulness measurements and an onscreen self-rating on the Karolinska sleepiness scale (KSS).

### *Data analysis*

All analyses were carried out in Python open source programming language and in SPSS Statistics (IBM Corp.). Recordings were sampled at 512 Hz and band-pass filtered between 0.2 and 128 Hz, with a notch filter at 60 Hz. All channels were re-referenced to linked mastoids. Sleep stages were visually scored per 30-s epoch as N1, N2, N3 or REMS, according to standard criteria (Iber, 2007). Re-referenced traces were visually scanned for artefacts, and affected 30-s epochs were excluded from further analyses. Sleep cycles were visually delimited from the resulting hypnogram, each cycle containing successive N2, N3 and REMS stages. Because frontocentral midline regions show maximal delta and sigma power in NREMS, maximal delta and theta power in REMS (Tinguely et al., 2006), and high synchronization of NREMS oscillations (Möller et al., 2002; Staresina et al., 2015), we focused our analysis on electrodes Fz and Cz. Power spectra were obtained using Welch's method, with a 2-s Hanning window. Raw power spectra were normalized by dividing by the spectrum integral. For filtering, we used a 3<sup>rd</sup> order Butterworth filter applied once forward and once backward to correct the filter's phase shift effect, resulting in a zero-phase shift 6<sup>th</sup> order Butterworth filter. For sigma band analyses and spindle detection, adapted bands were delimited per participant, per channel and per experimental night by visual discernment of the largest peak between 10 and 16 Hz in

the power spectrum of all concatenated N2 epochs. The adapted sigma band for each channel and participant was taken as the 4 Hz-wide band centred at the peak averaged between both nights. Because oscillatory bands are trait-like (Finelli et al., 2001), the same adapted bands were used for both nights, whereas all other measures described here were carried out independently for each night, then compared. Delta, theta and gamma bands were less discernible by eye, so *a priori* bands were used for these oscillations: delta in NREMS (0.25-4 Hz), delta in REMS (1.5-3.5 Hz), theta (3.5-8 Hz) and gamma (50-100 Hz). Delta in NREMS and REMS are thought to be of different physiological origins, so different bands were adopted based on the literature (Bódizs et al., 2001; Massimini et al., 2004). The upper 0.5 Hz in REMS delta and the lower 0.5 Hz in theta were added for fuller spectral coverage.

#### *Discrete slow wave detection*

Discrete SW and spindle events were detected using automated algorithms. For automatic SW detection, the re-referenced signal for stages N2 and N3 was first band-pass filtered between 0.1 Hz and 4 Hz, and SWs were detected according to the following criteria: (1) a negative zero-crossing followed by a positive zero-crossing 0.3-1.0 s later, (2) a negative zero-crossing within 1.0 s of the positive zero-crossing detected in criterion 1, (3) a minimum voltage lesser or equal to -80  $\mu$ V and (4) a peak-to-peak amplitude greater or equal to 140  $\mu$ V. These criteria were based on Mölle et al. (2002; criteria 1 and 3) and Massimini et al. (2004; criteria 1, 3 and 4). The algorithm was visually validated. The negative zero-crossings delimited the SW beginning and end. SW power was taken as the root-mean-square (RMS) value over the entire SW.

#### *Discrete spindle detection*

Automatic spindle detection was based on Mölle et al. (2011). To detect spindles, the re-referenced signal for stages N2 and N3 was band-pass filtered within the adapted band specific to each participant and channel. Artefacts in the filtered signal were removed by replacing amplitude values beyond 10 SD with the filtered signal mean. The RMS was then calculated at each data point of the filtered signal using a 0.2-s sliding window, and the resulting RMS signal was smoothed with a moving average of 0.2 s. Spindles were detected on the smoothed RMS signal where RMS values exceeded 1.5 SD uninterrupted for 0.5-3 s. Longer and shorter rises in power were rejected. The threshold crossing points delimited the spindle beginning and end. Spindle power was taken as the average of the smoothed RMS over the duration of the spindle. SW and spindle density were defined as the number of events per 30-s epoch of N2 and N3.

Duration, RMS and peak-to-peak amplitude were calculated for each individual oscillatory event where applicable, and then averaged per participant.

#### *Discrete detection-based cross-frequency coupling*

To quantify the synchronization between SWs and spindles, we constructed two event correlation histograms. For both, we divided all SWs into four quadrants: (1) from negative zero-crossing to negative peak, (2) from negative peak to positive zero-crossing, (3) from positive zero-crossing to positive peak and (4) from positive peak to negative zero-crossing. Next, for the first event correlation histogram, the number of spindles beginning in each SW quadrant was counted and expressed as a percentage of the total number of detected spindles for the whole night. For the second histogram, the spindle voltage minimum was used instead of the spindle beginning as a temporal marker of spindle occurrence. In a third analysis, average adapted sigma power was calculated over the entire SW (irrespective of quadrants). These analyses were carried out for all NREMS and for NREMS period 1 only (i.e. NREMS in sleep cycle 1). The advantage of this event-based synchrony analysis over the spectral-based PAC analyses described below is twofold: (i) it allows temporally precise segmentation of the SW, based on detected peaks, troughs and zero-crossings, rather than fitting the EEG trace to a modulated sine wave, and (ii) signal-to-noise ratio is improved by ignoring any delta or sigma power not meeting the criteria for SW or spindle detection (e.g. maximum and minimum duration, minimum power).

#### *Phase-amplitude coupling*

As a numerical index of PAC, we employed the modulation index (MI) described by Tort et al. (2010), implemented in Python based on Matlab (Mathworks Inc.) scripts shared with us by Adriana Tort. To obtain the MI for nesting frequency  $f_p$  and nested frequency  $f_A$ :

- (1) The re-referenced signal  $s(t)$  was band-pass filtered at both frequency ranges, yielding  $s_{fp}(t)$  and  $s_{fA}(t)$ .
- (2) The standard Hilbert transform was then applied to  $s_{fp}(t)$  and  $s_{fA}(t)$ , yielding analytic signals  $s_{fpa}(t)$  and  $s_{fAa}(t)$ , respectively.
- (3) The instantaneous phase of  $s_{fpa}(t)$  was extracted, providing the phase time series  $\phi_{fp}(t)$ , and the absolute value of  $s_{fAa}(t)$  provided the time series of the amplitude envelope  $s_{fAm}(t)$ . These were combined into the composite signal  $\phi_{fp}(t), s_{fAm}(t)$ , which indicates the absolute amplitude of  $f_A$  at every phase of the  $f_p$  oscillation.

- (4) We then binned  $\phi_{fp}(t)$  into 18 phase bins, each spanning  $\pi/10$ , or  $20^\circ$ , and computed the mean amplitude of  $s_{fAm}(t)$  per phase bin. The choice of 18 bins balances precision with computational savings.
- (5) The mean amplitudes per bin were normalized by dividing them by the sum over all phase bins.
- (6) The MI was obtained by applying the following formula, derived from the Kullback-Leibler divergence:

$$MI = \frac{\log(N) - \sum_{j=1}^N P(j) \log [P(j)]}{\log (N)}$$

where  $P(j)$  is the normalized distribution of mean amplitudes per bin, and  $N$  is the number of phase bins.

- (7) Finally, the MI was natural log-transformed for linear statistical analysis.

The MI formula offers a normalized metric of the dissimilarity between the distribution of interest and a uniform, or flat, distribution, and expresses it as a fraction of the maximum possible dissimilarity  $\log(N)$ . Note that a flat distribution of mean amplitudes per phase bin would evidence a complete absence of PAC, and would yield an MI of 0. SW to adapted sigma MI was calculated for stage N2 only, stage N3 only, and stages N2 and N3 combined, and for NREMS period 1 only and all NREMS combined. In REMS, two nesting frequencies were examined: delta (1.5-3.5 Hz) and theta (3.5-8 Hz). MI was calculated between these bands and gamma (50-100 Hz) as the nested band, for REMS period 1 only and all REMS combined. MI was calculated first per 30-s epoch, then averaged. In parallel with these analyses, average power in each of the concerned bands was calculated: delta (0.25-4 Hz) and adapted sigma power was taken for N2 only, N3 only, and N2 and N3 combined, and for NREMS period 1 only and all NREMS concatenated; and delta (1.5-3.5 Hz), theta and gamma power were taken for all REMS concatenated. We selected NREMS period 1 because of the greater delta activity in this period, and because it is more proximate to the learning event. Furthermore, prior studies relating sleep oscillations to learning did so mainly in the first NREMS period (Gais et al., 2002; Moroni et al., 2008). We chose to use all REMS periods together because even though the first REMS period is more proximate to the learning task, it is too short for a meaningful analysis.

Aru et al. (2015) recommend that PAC detection be underpinned by a rise in power in the nesting rhythm. To this end, we also performed a power-triggered analysis, with NREMS delta-sigma MI measured strictly over concatenated SW-concurrent signal. This ensured that significant power was always present in the phase-giving delta band. For PAC during REMS, we used a detection algorithm for delta and theta (the phase-giving signals) that was identical to the

spindle detection algorithm described above, with the exception that no maximum duration was imposed, and delta or theta were used for filtering instead of adapted sigma. Signal concurrent with detected delta or theta oscillatory trains was then concatenated, and delta- or theta-gamma MI analysis was performed over the concatenated trace. As was done for detected SWs and spindles, we calculated mean duration, density and average RMS for detected oscillatory trains in REMS. For the power-triggered analysis, we focused on NREMS period 1 for delta-sigma coupling, and all REMS periods concatenated for delta-gamma and theta-gamma coupling.

### *Phase analysis*

The MI expresses the coupling strength between two frequencies, but not their phase relationship. For example, a clustering of gamma power at the theta peak and an equal clustering of gamma power at the theta trough will result in equal MIs. Yet, phase dynamics appear to be functionally important in the brain (O'Keefe and Recce, 1993) and may be related to learning. Using the mean amplitudes per phase bin obtained in step 4 of the power-triggered MI analyses, we examined the effects of learning on phase dynamics by comparing the phase-amplitude plots directly between experimental nights, in Fz and Cz. Instead of normalizing with respect to the sum over all phase bins as in step 5 of MI analysis, we normalized with respect to the average RMS of the 5-minute quiet wakefulness recording made just prior to the pre-sleep task. This normalization corrects for EEG characteristics of the participant and the recording, as well as for effects of the task on subsequent EEG characteristics. We define the coupling phase as the  $f_p$  phase bin gathering the maximal  $f_A$  mean amplitude.

### *Comodulogram*

To further explore PAC dynamics during sleep, we employed a log-based comodulogram. The PAC comodulogram is a heat map of MI values at different combinations of phase (x-axis) and amplitude (y-axis) frequencies, i.e. it expresses the comodulation of two frequency ranges. Three considerations informed its design: (i) PAC can only be effectively detected if the bandwidth of the nested frequency  $\Delta f_A$  is at least double the centre value of the nesting frequency  $f_p$  (i.e.  $\Delta f_A \geq 2f_p$ ; Aru et al., 2015); (ii) there are inter-individual differences in the band limits of physiological EEG oscillations (Finelli et al., 2001); and (iii) the bandwidths of physiological oscillations are linearly distributed on a natural logarithmic scale (Buzsáki and Draguhn, 2004; Buzsáki and Mizuseki, 2014). In light of these considerations, the comodulogram was constructed as follows:

- (1) The adapted sigma centre frequencies  $f_\sigma$  were averaged over all participants, yielding  $\bar{f}_\sigma$ .

- (2) A progression of centre frequencies were generated, each separated by a distance of 0.6 and with a bandwidth of 0.6 on the natural logarithmic scale, spanning from ~0.5 Hz to ~30 Hz, such that it coincided with  $\bar{f}_\sigma$ . This progression provided the average nesting (phase-giving) frequency bands, with logarithmically increasing bandwidths presumably more faithful to brain oscillatory dynamics (iii). The choice of a step of 0.6 balances precision with computational savings.
- (3) The progression in (2) was extrapolated for ~10 Hz to ~128 Hz to provide average nested (amplitude-giving) centre frequencies.
- (4) Using the same method as in (2), a progression of nesting centre frequencies were generated for every participant according to their individual  $f_\sigma$ , thus adjusting to individual differences in oscillatory band-limits (ii).
- (5) As in (2-3), the progression in (4) was extrapolated to create the adapted nested frequencies.
- (6) MIs were computed using each individual's adapted nesting and nested frequencies, but instead of using fixed bandwidths for the nested frequencies, a dynamic bandwidth was imposed, such that the nested frequency bandwidth was always double the upper limit of the nesting frequency band. This ensured that the PAC bandwidth rule (Aru et al., 2015) was not violated (i).
- (7) MIs were log-transformed and then normalized with respect to the mean of all log-transformed MIs for that recording.
- (8) Normalized log-transformed MIs were then averaged among participants and represented on a heat map with the average nesting and nested frequencies from (2-3) on respective x and y axes.

As the comodulogram is computationally demanding, it was applied to the Cz signal only. All epochs of the relevant stage and cycle were concatenated for analysis, as an epochwise analysis would have been computationally onerous. Four comodulograms were generated per participant in step (7): learning night NREMS period 1, learning night REMS, control night NREMS period 1 and control night REMS.

### *Statistics*

Statistical analyses relied on three general linear models. Model 1 was an analysis of covariance (ANCOVA) with a repeated measures factor "Task" for the type of cognitive task, learning or non-learning, performed before (and after) sleep. The dependent variable (DV) was the sleep parameter of interest (i.e. absolute and relative MI and oscillatory parameters). This model

examined the effect of an intensive learning opportunity on subsequent sleep characteristics. Model 1 also took into account age as a covariate, recorded within two decimal places. Our limited sample size constrained us to using only one covariate, and age is at once known to affect sleep characteristics and, through its correlation with education (in our sample,  $r = 0.67$ ,  $p = 0.033$ ), to enhance learning ability. As such, we supposed age would account for maximal error in our variables of interest among participant characteristics. Model 2 was a multiple regression with age and the sleep parameter of interest as independent variables (IV). The DV was the overnight change in performance on the learning task, termed “Gains”, defined as the number of word pairs recalled post-sleep minus the number recalled pre-sleep, divided by the total number of word pairs presented. This model tested the influence of sleep parameters on overnight memory maintenance. Multiple regression was again employed in Model 3, taking age and the pre-sleep memory performance score as IVs and the sleep characteristic of interest as the DV. This last model aimed to test the effect of the amount of successful pre-sleep encoding on subsequent sleep characteristics. For Models 2 and 3, the absolute MI and power analyses were complemented by analyses of relative MI and power, wherein the relative value was taken as the learning night value divided by the control night value. In this way, relative MI and relative power provided indices of the relative change in these parameters following an intensive learning opportunity. All three models were applied to oscillatory parameters (duration, RMS, amplitude, density); spindle counts per SW quadrant; sigma power per quadrant; average sigma power over SWs; absolute and relative power-triggered log-normalized MIs per band, stage and cycle; and absolute and relative power values per band, stage and cycle. For the phase analysis, Model 1 was used to determine whether “Task” predicts mean amplitudes per phase bin, with age as covariate, with the added fixed factor “Phase bin”.

Using results of the log-based comodulogram, we undertook a systematic comodulation analysis. Differences between experimental nights were examined using paired samples  $t$ -tests, comparing every learning night MI value with its control night counterpart, for both NREMS period 1 and REMS separately. For both stages, in order to visualize the topography of statistical difference probability between learning and control nights, we generated a comodulogram of mean MI differences and a corresponding comodulogram of  $p$ -values. To detect sleep stage differences in coupling, we averaged corresponding MIs from learning and control nights, and used  $t$ -tests to compare each average between REMS and NREMS period 1. Again, a mean difference comodulogram and a  $p$ -value comodulogram were generated to visualize coupling difference topography.

Because this was an exploratory study, and because we targeted our analysis to certain oscillatory bands we believed to be meaningful based on prior studies, we set  $\alpha$  to 0.05 for all CFC analyses. In the stage difference comodulogram, we expected larger differences, so  $\alpha$  was set to 0.01 instead.

## Results

### *Participant sample*

We recorded 18-channel scalp EEG from 10 participants as they slept following either a learning task or a non-learning control task. Out of 257 responders to the online advertisement, 156 were successfully screened by telephone. Among those deemed eligible, 45 were interviewed in person and 36 were screened by overnight PSG. Four participants dropped out for personal reasons, and a fifth because of an allergic reaction to the PSG equipment. A further three were taken out of the study for not keeping appointments or for breach of protocol. Lastly, two participants' data were excluded from analysis because of poor sleep on experimental nights, due to illness. The final sample of 27 participants were recorded in three cohorts. The first pilot cohort of 13 participants were tested under a different design from the rest, and their results are not presented here. The second cohort of 10 participants (5 female) are the final sample presented in this paper, and are from now on referred to as the participant sample. The third cohort of four participants, recorded later on, will soon be combined with the second for further analysis. Characteristics of the participant sample, including age, number of years of education and questionnaire scores, are presented in Table 1. Participants' sleep quality and duration were normal on both experimental nights (Table 2), with the exception of one participant who experienced pain from the onset of an acute medical condition. In this case, the night was cut short after two sleep cycles. This duration was sufficient for the participant's data to be retained. All participants slept for at least two cycles each night. Epochwise artefact rejection resulted in the exclusion of an average of 11.6 % ( $SD = 6.3$  %) of 30-s epochs per recording, including epochs of waking mobility.

### *Learning task*

In the learning task, participants recalled an average of 59.8 (49.8 %) ( $SD = 34.1$ ; 28.4 %) out of 120 words on the pre-sleep test, and 59.5 (49.6 %) ( $SD = 35.0$ ; 29.1 %) on the post-sleep test (Table 3). The overnight change in performance, or gains, ranged from forgetting 6 words to remembering an additional 3 words, with a mode at remembering one additional word. Five

participants improved their score overnight and three decreased in score, such that there was no statistically significant change in score ( $p > 0.05$ ).

### *Power spectra*

Power spectral densities were computed across all electrodes for delta (0.5-4 Hz) and sigma (10-16 Hz) in NREMS, and delta (1.5-3.5 Hz) and theta (4-8 Hz) in REMS (Fig. 2). Cz and Fz showed the greatest concentration of power in these bands, and so were chosen for all further analyses. Spectral distributions at Cz for each participant, stage and task condition are shown in Figures 3 and 4. Strong NREMS sigma peaks are visible in all participants (Fig. 3), while REMS theta peaks are visible in 5 out of 10 participants (Fig. 4). Adapted sigma bands were detected from stage N2 power spectral peaks (Fig. 5). Peaks for each channel and participant agreed closely between experimental nights ( $r = .87$ ,  $p = .00093$ ) (Fig. 6). We then compared spectral power between experimental nights (Model 1). We split NREMS into N2 and N3, and checked for differences in delta (0.25-4 Hz) and adapted sigma. In REMS, we checked for differences in delta (1.5-3.5 Hz), theta (3.5-8 Hz) and gamma (50-100 Hz). In all cases, we applied the analysis either to all epochs of the stage, or only to epochs in cycle 1. Because we had no *a priori* assumptions about power differences, we used the more stringent Bonferroni method to correct for multiple comparisons ( $\alpha = 0.0125$ ; 4 related tests per frequency band). No statistically significant differences were detected between learning and control nights ( $p > 0.0125$ ; NREMS: Table 4; REMS: Table 5), although a low  $p$ -value ( $p = 0.049$ ) was obtained for normalized delta power in REMS, with the control night value exceeding the learning value by a considerable effect size ( $d = 0.54$ ). We then probed for effects of learning night spectral power on overnight gains in the learning task (Model 2). In this model, we also looked at effects of relative power (ratio of learning night to control night power); we corrected  $\alpha$  accordingly ( $\alpha = 0.0125$ ). There were no statistically significant correlations ( $p > 0.0125$ ; NREMS: Table 6; REMS: Table 7). Lastly, Model 3 was applied to all absolute and relative power values to assess the effect of successful pre-sleep encoding. Again, no statistically significant correlation was found ( $p > 0.0125$ ).

### *Discrete oscillatory events*

Discrete spindles and SWs were successfully detected in stages N2 and N3 on channels Fz and Cz using our custom detection algorithms, detailed in Methods. Delta and theta trains were detected in stage REMS on Fz and Cz using an algorithm similar to the spindle detector. Event densities per 30-s epoch are shown in Table 8. SW density showed the greatest variability; other

event densities were moderately variable within and between participants. None of the densities were correlated with age ( $p > 0.05$ ). Average oscillatory parameters per participant (density, duration, RMS and amplitude) are shown in Tables 4 (NREMS) and 5 (REMS). No significant differences were found between experimental nights, using Model 1 with a corrected alpha of  $\alpha = 0.0125$  (4 related tests per frequency band), although low  $p$ -values for SW RMS ( $p = 0.049$ ) and amplitude ( $p = 0.050$ ) indicate a possible increase in SW power in the learning night, with a minimal effect size (Cohen's  $d = 0.19$  and  $d = 0.04$ , respectively; Tables 4 and 5).

Judging by the same corrected alpha of  $\alpha = 0.0125$ , Model 2 did not reveal any significant correlation between absolute or relative oscillatory parameters and gains (Tables 6 and 7, respectively). Still, the recurrence of marginally significant ( $p < 0.05$ ) event density correlations in REMS indicate a possible negative relationship. Greater delta train density on Fz and Cz and theta train density on Cz were associated with overnight decreases in performance, on the order of  $-2$  to  $-6$  percentage points (pp) per additional unit of relative density. Similarly, overnight gains showed a marginally significant negative correlation with NREMS SW RMS at Fz ( $F = 5.89$ ,  $p_{RMS} = 0.024$ ) and Cz ( $F = 3.26$ ,  $p_{RMS} = 0.089$ ), with large effect sizes of  $-32$  pp ( $SD = 11$  pp) and  $-20$  pp ( $SD = 10$  pp) per unit of relative power increase, respectively. Another marginally significant correlation was detected between gains and delta train RMS ( $F = 4.99$ ,  $p_{RMS} = 0.036$ ), with a positive effect size of  $4.1$  pp ( $SD = 1.6$  pp) per relative power unit. With the exception of this last correlation, all correlations detected between gains and oscillatory parameters, namely delta and theta densities, and delta and SW power, were negative. However, given the high  $p$ -values and small effect sizes (except for SW RMS), they are to be considered only tentatively. A closer look at the SW RMS data (Fig. 7) indicates the correlation was driven by an outlier.

The relationship between successful pre-sleep encoding and oscillatory parameters was investigated using Model 3. Pre-sleep score, expressed as a ratio, was positively correlated with the average theta train absolute duration on Fz during REMS ( $F = 8.17$ ,  $R^2 = 0.70$ ,  $b = 0.22$ ,  $p_{dur} = 0.015$ ). According to these results, every 10 pp increase in baseline score was associated with a  $0.022$  s ( $SD = 0.06$  s) increase in theta train duration, amounting to only a fraction of a theta cycle. As such, this finding is probably trivial.

The trough-triggered grand average of all detected spindles (Fig. 8) clearly displays the coupling of spindles to the ascending phase (up-state transition) of the SW. The synchrony between detected SWs and spindles was quantitatively assessed first by counting the number of spindles beginning in each quadrant of the SW. No significant difference in quadrant spindle counts was detected between experimental conditions, nor were the counts predictive of

performance gains. The spindles were then counted instead using their amplitude minimum as a temporal marker, and again no significant result was found. Next, the average adapted sigma envelope over each SW was averaged per participant, normalized with respect to the participant's pre-sleep, pre-task, 5-min quiet wakefulness recording, and averaged for each experimental night across participants. The result is plotted in Figure 9. The average power over the SW trough was compared between learning and control nights using Model 1; no significant difference was detected. We then used Model 2 to probe for a relationship between relative adapted sigma power over the SW trough and performance gains. A significant negative correlation was detected ( $F = 5.48$ ,  $p_{power} = 0.029$ ), meaning that greater sigma power over the SW trough (up-state) in the learning night was associated with worse overnight memory stabilisation.

#### *Phase-amplitude coupling with a priori bands*

PAC on Fz and Cz was quantified using the MI, applied to delta (0.25-4 Hz) with adapted sigma in NREMS, delta (1.5-3.5 Hz) with gamma (50-100 Hz) in REMS, as well as theta (3.5-8 Hz) with gamma in REMS. Average values were obtained by calculating the MI for each 30-s epoch within a stage and cycle, then averaging. For all NREMS analyses, epochs from stages N2 and N3 were combined. For each band pair, we obtained average MIs for all cycles together, and for the first cycle only.

Raw MIs were lognormally distributed (Fig. 10). Accordingly, all MIs were log-transformed for Gaussian-based analysis. No significant differences between learning and control nights were identified for either band pair using the Model 1 ANCOVA with  $\alpha = 0.05$  (Table 9 and Fig. 11). Delta-sigma MI on Cz during NREMS period 1 was slightly greater in the learning night than in the control night, with a trend to significance ( $F = 4.94$ ,  $p = 0.057$ ) and an appreciable effect size ( $d = 0.29$ ). This result was not reflected in Fz. Next, the Model 2 regression was applied to relative MIs (learning night MI divided by control night MI), to determine the predictive strength of MI on performance gains (Table 10). Two statistically significant correlations were identified on Fz. First, delta-sigma relative MI in NREMS period 1 was highly predictive of gains ( $F = 11.42$ ,  $p_{MI} = 0.004$ ), with a large effect size of 51 pp ( $SD = 12$  pp) gains per unit increase in relative MI (Fig. 12). No such effect was detected for all NREMS periods combined. Second, theta-gamma MI in REMS was predictive of gains ( $F = 8.91$ ,  $p_{MI} = 0.009$ ), but with the inverse relationship; a unit increase in relative MI corresponded with a 47 pp ( $SD = 13$  pp) decrease in gains (Fig. 13). A third correlation was found on Cz, whereby delta-gamma MI in REMS was negatively related to gains ( $F = 4.68$ ,  $p_{MI} = 0.041$ ), with a 35 pp ( $SD =$

14 pp) decrease in gains per unit increase in relative MI. As for the remaining two REMS PAC measures, delta-gamma MI on Fz and theta-gamma MI on Cz, although their  $p$ -values were above threshold, they were relatively low ( $p < 0.20$ ), and their effect sizes were similar in direction and magnitude to their statistically significant counterparts. From these data, it would seem that declarative memory consolidation in sleep is at once concurrent with an increase in early NREMS frontal PAC and a decrease in REMS frontal and central PAC. Lastly, Model 3 regression was applied to log-transformed relative MIs to probe the relationship between successful pre-sleep encoding and subsequent sleep PAC. No statistically significant effect was detected for either of the three band pairs (Table 11).

We sought to corroborate these findings with power-triggered MI, a more stringent measure of PAC. In Model 1 (Table 12 and Fig. 14), we found a statistically significant increase in control night delta-sigma MI compared to the learning night in NREMS period 1 on Fz ( $F = 6.51$ ,  $p = 0.034$ ). However, the effect size is negligible (Cohen's  $d = 0.091$ ). Relative power-triggered MIs were then inserted into Model 2 to corroborate the delta-sigma, delta-gamma and theta-gamma correlations with gains. The correlations could not be reproduced, nor was any other correlation detected (Table 13). Model 3 regression on relative power-triggered MIs was equally ineffective.

### *Phase analysis*

Coupling phase differences between experimental nights were investigated by comparing binned mean amplitudes from the *a priori* PAC analysis. We examined mean adapted sigma amplitudes binned by delta phase, in NREMS period 1 only. Mean amplitudes were log-transformed and normalized, and sorted into 18 phase bins (Fig. 15). The averages for each experimental night across participants are presented in Figure 16. From these phase-amplitude plots, delta-sigma coupling phase seems smeared to the right in the learning night compared to the control night, with the greatest learning-related increase situated in the latter half of the delta wave rising slope (90-180°). A two-way ANCOVA was conducted to find statistically significant differences in mean amplitude between experimental nights (Task) and phase bins (Phase), controlling for age. To simplify the analysis, mean amplitudes were averaged into two phase bins: the delta rising phase (trough to peak, or down- to up-state) and falling phase (peak to trough, or up- to down-state). While there was no effect of Task ( $F = 1.07$ ,  $p = 0.33$ ) or Phase ( $F = 4.11$ ,  $p = 0.077$ ) for Fz, there was a statistically significant interaction between Task and Phase ( $F = 13.91$ ,  $p = 0.006$ ), whereby the difference between rising phase and falling phase mean amplitudes was more pronounced on learning nights than on control nights (Fig. 17). This

interaction was mirrored in Cz ( $F = 7.75$ ,  $p = .024$ ), while Task ( $F = 1.07$ ,  $p = 0.33$ ) and Phase ( $F = 3.24$ ,  $p = 0.11$ ) showed no effect. Relative log-transformed mean amplitudes (learning divided by control) were then correlated with performance gains using regression Model 2 (Table 14). Relative mean amplitudes over the SW rising phase on Cz were predictive of an overnight performance decrease ( $F = 5.35$ ,  $p_{MA} = 0.031$ ), with unit increases in relative mean amplitude concomitant with a 21 pp ( $SD = 78$ ) decrease in gains. Other relative mean amplitudes did not show a statistically significant prediction, although it is worth noting that their effect sizes agree with the statistically significant result in both direction and magnitude.

### *Comodulogram*

In the comodulogram analysis, we systematically scanned phase and amplitude frequency bands for PAC differences between experimental nights, on Cz only. Four comodulograms were produced per participant: NREMS period 1 and all REMS periods in learning and control night conditions. A sample participant's comodulograms for NREMS and REMS are shown in Figure 17. Final MI values in each comodulogram were obtained from raw MIs by first log-transforming them, then normalizing them with respect to the comodulogram average. We averaged each MI across participants to obtain mean comodulograms for each of the four conditions. Comparisons of MIs between learning and control nights for NREMS and REMS are shown in Figures 19 and 16, respectively. Reported frequencies for the comodulogram are extrapolated from the average adapted sigma centre frequency; actual frequencies varied among participants, according to their visually selected adapted sigma centre frequency.

Significant differences of particular interest were detected in the REMS comodulogram (Table 15, Fig. 20). A cluster of statistical significance is visible in Figure 20 in the theta to beta/gamma range, whereby learning night MI was greater than control night MI. The cluster ranged from 4.3 Hz to 5.8 Hz in the phase band, with 22.1 Hz to 37.6 Hz in the amplitude band. The greatest difference was at  $f_p = 4.3-5.0$  Hz with  $f_A = 27.6-37.6$  Hz ( $p = 0.0011$ ). Three other points in the cluster were at  $f_p = 4.3-5.0$  Hz with  $f_A = 22.1-33.1$  Hz ( $p = 0.048$ ),  $f_p = 5.0-5.8$  Hz with  $f_A = 22.1-33.1$  Hz ( $p = 0.0196$ ) and  $f_p = 5.0-5.8$  Hz with  $f_A = 27.6-37.6$  Hz ( $p = 0.087$ ). A fifth significant MI difference was detected in the theta-gamma range, but slightly removed from the cluster, at  $f_p = 6.8-7.8$  Hz with  $f_A = 30.0-45.7$  Hz ( $p = 0.014$ ). Thus, theta-beta/gamma coupling was increased centrally in REMS after a learning task. A second cluster of significance is visible in the delta-gamma range; however, the direction of the effect is inconsistent (see Table 15).

In NREMS (Table 14, Fig. 19), we found that control night MI was significantly greater than learning night MI at  $f_p = 6.8-7.8$  Hz with  $f_A = 72.4-88.0$  Hz ( $p = 0.012$ ). A nearby point

corroborates this finding, at  $f_p = 6.8-7.8$  Hz with  $f_A = 51.6-67.2$  Hz ( $p = 0.024$ ). Contrary to REMS, theta-gamma seems to be decreased centrally in NREMS after a learning task. Another isolated significant difference was located in the delta-gamma range at  $f_p = 1.8-2.0$  Hz with  $f_A = 56.4-62.4$  Hz ( $p = 0.029$ ), whereby learning night MI was greater than control night. This finding is difficult to corroborate because of the comodulogram's sparseness in low-to-high frequency coverage. Because of the choice of a dynamic bandwidth in this comodulogram, MIs with low phase frequencies are paired with narrow amplitude bandwidths (as these double the phase frequency maximum). As a result, some high amplitude frequencies are omitted from analysis at low phase frequencies, such that we do not obtain a full picture of low-to-high frequency PAC.

To characterize coupling dynamics across sleep stages, we also compared the NREMS and REMS averages. We did this by averaging MIs between experimental nights for each stage. Difference values (REMS minus NREMS) are shown in Figure 21. Four clusters are visible. First, low delta (~1 Hz) to sigma (12-16.5 Hz) coupling is greater in NREMS ( $p < 0.01$ ), as would be expected. But surprisingly, high delta (2.75-4 Hz) to alpha/sigma/beta (9-18 Hz) coupling is greater in REMS ( $p < 0.01$ ). Sigma (12.3-14.3 Hz) to beta/gamma (14-43 Hz;  $p < 0.05$ ) also appears increased in NREMS. Delta comodulation of alpha (8-12 Hz) is greater in NREMS as well ( $p < 0.01$ ). Lastly, low delta (~1.5 Hz) to beta (27-30 Hz) and gamma (36-39 Hz) were greater in REMS ( $p < 0.05$ ). Again, the low- to high-frequency sparseness of the comodulogram makes this last cluster difficult to interpret.

## Discussion

By recording scalp EEG while human participants slept following an intensive declarative learning opportunity, this study provides experimental evidence of an effect of learning on sleep CFC, and contributes correlative evidence of a relationship between sleep CFC and memory consolidation. The findings are consistent with counterbalancing effects of NREMS and REMS CFC on declarative memory consolidation. In early NREMS, frontal increases in delta-sigma PAC with respect to the non-learning control night were predictive of better overnight word pair retention. Conversely, in REMS, frontal theta-gamma and central delta-gamma PAC increases predicted worse overnight retention. Coupling intensification not only preceded retention, but also succeeded encoding. After learning tasks, compared to after control tasks, we observed coupling strength increases in the vicinity of these same rhythm pairs. In NREMS period 1, delta-sigma PAC was increased at Cz, albeit with marginal statistical significance, and in REMS,

narrowband delta-to-gamma PAC and wideband theta-to-beta/gamma PAC were both markedly increased at Cz.

Importantly, oscillatory interactions predicted retention independently of the individual characteristics of their constituent rhythms, which themselves showed weak or absent associations. Here, the link between sleep and memory is an emergent property of its system of rhythms. Cox et al. (2012) came to a similar conclusion from their data showing that spindles better predicted memory performance when occurring in conjunction with SWs in stage N3.

In comparing the raw comodulograms in Figure 18 with the respective difference comodulograms of Figures 19 and 20, it is interesting to note that the distribution of learning-related changes in PAC bears little resemblance to the absolute PAC strength distribution. This may indicate that learning-dependent PAC is weak compared to other PAC processes in the brain.

#### *NREMS CFC and learning*

Previous behavioural studies have identified SWs and spindles as individual mechanisms of sleep-dependent memory consolidation. We submit that if changes in these oscillations contribute to memory consolidation, it is perhaps by the intermediary of their synchronization. It would follow that SW-spindle CFC may be a more specific biomarker of successful memory consolidation. Our secondary results bear this out, showing effects of learning on parameters of individual oscillations that were weak in comparison to their effects on PAC, and no effect of these parameters on retention. This contrasts with studies reporting effects of word pair learning on spindle density (Gais et al., 2002) or correlations between spindle density and overnight word pair retention (Gais et al., 2002; Schabus et al., 2004; Cox et al., 2012). But a closer comparison with these studies reveals important differences. Two of these studies (Gais et al., 2002; Schabus et al., 2004) counted spindles in stage N2 only and the other (Cox et al., 2012) in stage N3 only. The present study instead aggregated spindles from stages N2 and N3. In addition, we normalized learning night spindle counts with respect to the control night using a ratio (learning divided by control), whereas previous studies used absolute (Gais et al., 2002; Schabus et al., 2004; Cox et al., 2012) or difference (Schabus et al., 2004) measures. Lastly, one of these studies (Schabus et al. 2004) detected effects of spindle activity on retention by dichotomizing their participant sample into spindle enhancers and non-enhancers and applying an analysis of variance, whereas we applied a regression to the continuous spindle count ratios. It may be that the measures employed in these other studies were more sensitive to spindle effects. Nonetheless, we believe that our method of applying multiple regression to the continuous

distribution of normalized (learning divided by control) spindle densities, in all NREMS stages containing spindles, constitutes an at once controlled and comprehensive assessment of spindle effects. Normalization with respect to control values is particularly important. Because most brain dynamics are log-normal and hence the result of many multiplicative effects (Buzsáki and Mizuseki, 2014), we should expect that behaviour-related changes are also multiplicative. Normalization returns multiplicative changes to an additive standard, unbiased by baseline differences.

As to SW parameters, our findings are consistent with a stereo EEG study by Moroni et al. (2008) that reported no effect of word pair learning on cortical SW power during sleep (although SW RMS at Fz was marginally significantly increased after learning in our data, in agreement with findings from Mölle et al., 2009). Moroni et al. (2008) did show effects for motor learning. Similarly, a study led by Tononi found SW power increases following motor learning, which were topographically bound to regions recruited by the task, and which were correlated with next-day performance (Huber et al., 2004). The synaptic homeostasis hypothesis suggests that SWs contribute to the renormalization of synaptic strengths following net potentiation from daytime learning (Tononi and Cirelli, 2006; Tononi et al., 2014). Taking this view, it may be that motor learning opportunities are sufficiently uncommon in the typical research participant's day, and motor synapses so seldom modified, that any potentiation resulting from a motor learning task can stand out as SWs in the sleeping brain. In contrast, the synaptic effects of a declarative learning task may be drowned out by the ubiquitous declarative learning episodes of a typical day (e.g. talking to a friend, reading, watching television). In our task, we attempted to compensate for this extraneous learning by presenting a large amount of information. But insofar as it affects SW power, the amount of information may still have been insufficient to stand out against the background of the day. Regarding effects of SW parameters on memory consolidation, we again found no correlation. Previous work has established a causal relationship between SWs and the improvement of overnight recall (Marshall et al., 2004; Marshall et al., 2006). These studies show that artificially inducing or disrupting SWs alters memory consolidation, but they do not speak to the predictive power of baseline SW parameters in a natural setting. Our work shows that in an ecologically valid setting, endogenous variability in SW parameters is not predictive of memory performance.

Phase-amplitude coupling may provide a more sensitive marker of endogenous NREMS memory processes. As stated, in the first cycle of NREMS, adapted sigma power was more strongly tuned to delta phase following a learning task. Furthermore, delta-sigma relative PAC (RPAC; i.e. learning night PAC divided by control night PAC) in this same period strongly

predicted overnight change in recall performance (Fig. 12). This last finding is consistent across participants: those who increased their recall score overnight showed increased PAC in the learning night, and those whose score decreased also decreased in PAC. Similar to this, Niknazar et al. (2015) found that the timing of spindles during the SW up-state transition predicted better recall after a morning nap. We may surmise from these findings that the degree of synchronization of SWs and spindles (i) is variable, (ii) is modified by learning in prior waking and (iii) is correlated with successful recall of this information. As such, we offer delta-sigma RPAC in early NREMS as a potential biomarker of sleep-dependent memory consolidation.

An examination of the delta-sigma phase-amplitude distribution revealed a concentration of sigma power at the delta trough, reaching its peak during the rising phase (Fig. 16). Taking the delta trough as reflecting the SW up-state, these phase dynamics are suggestive of spindle triggering by SW onset (Contreras and Steriade, 1996; Steriade, 2006), with the spindle peak reached as the down-state transition begins. Past studies have observed similar phase coupling (Möller et al., 2002; Möller et al., 2011; Staresina et al., 2015). Comparing phase-amplitude plots between learning and control nights, we found that sigma power is smeared towards the right in the learning night, representing an extension of spindle power into the down-state transition. However, this trend was only visible in half of the participants. Möller et al. (2011) reports a similar observation, whereby learning enhanced the power of slow spindles (9-12 Hz) which occurred mostly at SW down-state transitions. Slow spindles were considered distinct from fast ones (12-15 Hz) in their analysis, whereas in the present study, sleep spindles were taken as a unitary phenomenon (Zerouali et al., 2014). In addition, in our discrete SW analysis, we found that greater sigma power during the SW up-state predicted worse retention post-sleep. In contrast with our results, Niknazar et al. (2015) reported that spindles occurring during up-state, not down-state, transitions were most predictive of successful declarative recall. It should be noted that both this study and Möller et al.'s (2011) used *a priori* bands for spindle detection, while the present study used adapted bands.

### *REMS CFC and learning*

As in NREMS, we observed no learning-induced changes in REMS oscillatory parameters, nor were these parameters significantly predictive of memory performance, although a marginally significant increase in normalized delta power was observed after learning in REMS. There is scant evidence linking theta or delta oscillatory parameters in REMS to declarative memory consolidation (Fogel et al., 2007). This study did not replicate findings from Fogel et al. (2007), showing a statistically significant theta power rise at Cz after word pair learning, compared to a

non-learning night. This may be due differences in spectral data analysis: Fogel et al. log-transformed the spectral data and made comparisons using absolute values, while we did not log-transform the data, and expressed it as a ratio of total spectral power for comparison. The optogenetic study by Boyce et al. (2015) demonstrated that hippocampal theta is necessary for contextual memory consolidation in the rat, but like the studies by Marshall and colleagues (2004; 2006) for SWs in NREMS, they say little about the impact of naturalistic variations in theta on successful memory encoding and retrieval.

To our knowledge, this study is the first to report associations between REMS CFC and cognition in humans or animals. Specifically, we found that theta (4-8 Hz) to beta/gamma (22-46 Hz) PAC was increased at Cz after a learning task compared to a non-learning task, while modulation of gamma (50-100 Hz) was unchanged. Furthermore, theta (3.5-8 Hz) to gamma RPAC at Fz, as well as delta (1.5-3.5 Hz) to gamma RPAC at Cz, both predicted decreased overnight retention. Previous intracranial EEG studies in humans have identified significant PAC in the delta-gamma (Clemens et al., 2009; Amiri et al., 2016) and theta-gamma (Amiri et al., 2016) ranges during REMS. Rodent studies also show strong theta-gamma PAC in REMS, comparable to, or even stronger than, that seen in waking locomotion (Montgomery et al., 2008; Scheffzük et al., 2011; Brankačk et al., 2012). None of these studies investigated learning effects.

#### *Differences in CFC by stage*

Perhaps unsurprisingly, there were some significant differences in CFC between NREMS and REMS (Fig. 21). As expected, delta-sigma coupling was much stronger in NREMS, but only for the lower end of delta (~1 Hz). High delta (2.75-4 Hz) to sigma PAC was instead decreased in NREMS. The coupling of spindles specifically to the slow oscillation (SO) frequency (~1 Hz; Steriade et al., 1993) is a common finding (Mölle et al., 2011; Staresina et al., 2015). From our data, it seems plausible that the SO acts as an attractor that pulls spindles away from high delta comodulation. Alternatively, high-delta to alpha/beta (9-18 Hz) may simply be enhanced in REMS. In future CFC work, it will be advantageous to consider low delta and high delta separately. Unexpectedly, low delta (0.75-2.25 Hz) to alpha (8-12 Hz) showed a strong increase in NREMS.

#### *Significance of sleep CFC for learning*

This work comprises a direct test of a widely held hypothesis in sleep and memory research, that newly learned memories are stabilized and integrated into existing knowledge networks through

the temporal orchestration of NREMS oscillations (Diekelmann and Born, 2010; Lewis and Durrant, 2011; Rasch and Born, 2013; Tononi and Cirelli, 2014). Our results support this notion. We have shown that the phase of the cortical SW biases the occurrence of thalamocortical spindles, and that the extent of this bias is at once increased by learning and predictive of successful retention. Importantly, these effects are independent of characteristics of their underlying oscillations, meaning that high-order oscillatory synchronization is critical for sleep-dependent memory consolidation. The coordination of electrical oscillations may provide windows of synchrony through which information is routed in the brain (Fries, 2005; Canolty and Knight, 2010).

With respect to memory, temporal segregation of neuronal activity may encode time and place in the brain. Sleep oscillations, especially hippocampal SPW-Rs, are thought to enact retrospective replays (Wilson and McNaughton, 1994; Rasch and Born, 2013), anticipatory “pre-plays” or simply “plays” of memories, embedded, interpreted and *mis en scène* within the brain’s larger knowledge network (Gupta et al., 2010; Tononi and Cirelli, 2014). These “memory plays” are organized at progressively longer scales by spindles and SWs (Staresina et al., 2015) and are thought to at once stabilize memories and integrate them with prior knowledge (Lewis and Durrant, 2011; Stickgold and Walker, 2013). Were memories of different places and times to be played haphazardly, or all at once, their neuronal activations would become intermingled and their features conflated. Unless memory plays are spatially segregated in the brain, which is highly unlikely given that memories combine aspects that recruit the entire brain (senses, emotions, language, semantic associations), they must be separated in time. Neuronal oscillations seem ideally suited to this task, by parsing neuronal activity into discrete packets that can code for when and where (Buzsáki, 2010).

In light of this discussion, we may paint the following speculative picture, in broad strokes. In NREMS, spontaneous, avalanche-like SW discharges in the neocortex trigger thalamocortical loop firing. The resulting pattern of potentiation queries the hippocampus into divulging the sparse cortical trace of an associated episodic memory. The activation of this trace, in consultation with ongoing cortical and thalamocortical activation from the SW, informs the next burst of thalamocortical loop firing, bookended by GABAergic inhibition from the thalamic reticular nuclei (Steriade et al., 1993). With each cycle of this waxing thalamocortical spindle, the cortico-hippocampal memory is played and replayed, each time generating new activation patterns in the wider knowledge network that are then fed back into the loop. Finally, the SW dissipates and the spindle wanes. Presumably, this results in the integration of the memory into the wider knowledge network, according to its correlation with existing cortical patterns, which

are sampled by the ongoing SW (Tononi and Cirelli, 2014). And perhaps by token of this integration alone, the memory is consolidated. Then, a new SW swells, a new thalamo-cortico-hippocampal loop emerges, and a new episodic memory is integrated. Critically, each SW is insulated in time, to ensure that temporally discontinuous memories do not become integrated and confused. Just as importantly, the spindle loop must occur during the SW so that the processing of the SPW-R-bound memory can be integrated into the SW-activated network. A spindle-SPW-R complex occurring out of synch with SWs, or too early or too late in a SW, may have less ongoing network activity with which to integrate its memory trace, leaving the trace difficult to access in waking life. In this way, SW-spindle CFC would be indispensable for sleep-dependent memory consolidation, in agreement with our data.

The picture for REMS CFC is less clear. Studies in awake humans have connected theta-gamma PAC to memory processes (Canolty et al., 2006; Sauseng et al., 2009; Axmacher et al., 2010; Kaplan et al., 2014; Sweeney-Reed et al., 2014), particularly in the formation of later-remembered versus later-forgotten declarative memories (Osipova et al., 2006; Staudigl and Hanslmayr, 2013; Lega et al., 2014). Rodent studies corroborate these findings (Shirvalkar et al., 2009; Tort et al., 2009). Theta-gamma PAC is thus emerging as an intraspecific marker of declarative memory formation (Canolty and Knight, 2010). In addition, hippocampal delta-gamma PAC has been related to exploration in humans (Jacobs, 2007). It is counter-intuitive, then, that theta-gamma or delta-gamma PAC should predict worse memory performance, as we report here. We suggest that the answer may lie in the vigilance state. Ongoing brain activity during wake is correlated with features of the environment, through perception and action, but it is not so in sleep (Tononi et al., 1996; Tononi and Cirelli, 2014). According to the synaptic homeostasis hypothesis, spontaneous activity throughout the sleeping cortex provides neurons with a comprehensive sampling of the brain's knowledge of the environment, one which it has acquired through its entire developmental and evolutionary history (Tononi and Cirelli, 2014). In this state, the integrative action of synaptic renormalization can heed both daytime learning and prior knowledge. If renormalization were to occur in wake, i.e. in correlation with the environment, the limited and biased knowledge of the present moment would exert undue influence on the brain's future state (Tononi and Cirelli, 2014). The opposite is true for episodic memory formation. Episodic memories store novel information in space and time dimensions, and should be formed in connection with the environment. If episodic memory formation processes were to be engaged during sleep, neuronal correlations inferred from the environment during wake (signal) would become mixed with random input from spontaneous activity (noise), resulting in spurious learning (Nere et al., 2013; Tononi and Cirelli, 2014). And so, if we take

theta- and delta-gamma PAC as markers of episodic memory formation, we should expect that their occurrence in sleep predict worse recall, and this is precisely what we have found in REMS.

Indeed, theta and gamma rhinal-hippocampal coherence in sleep are correlated with dream recall (Fell et al., 2006), indicating that theta and gamma in sleep are contributing to the formation of new episodic memories about sleep-specific activity (dreams), rather than to the consolidation of existing memories from waking life. The haphazard connections made during dream mentation, when they are consolidated, may weaken existing connections derived from waking experience. In terms of the present study, if a participant learned the word pair association “cup – sand”, for example, and later dreamt of having a cup of tea and madeleines with a well-dressed cuttlefish, and if this dream was consolidated, then in the morning, the word “cup” may elicit memories of tea, madeleines and cuttlefish which now compete with the target word “sand”.

Although we did not examine the relationship between NREMS theta-gamma or delta-gamma PAC and memory performance, we did detect a decrease in these couplings, as mentioned. In light of the preceding discussion, this decrease seems adaptive: PAC-mediated memory formation in NREMS would be deleterious. In REMS however, we observed the opposite: learning increased coupling. Why would such a mechanism be promoted in REMS if it erodes existing memories? And why is it ubiquitous in animal REMS? The purpose of REMS is itself unclear (Jouvet, 1998; Siegel, 2005; Poe et al., 2010; Rasch and Born, 2013; Tononi and Cirelli, 2014). An intriguing possibility was posed by Stickgold et al. (2001). Given that in REMS, hippocampal outflow is inhibited (Buzsáki, 1996) and limbic activity enhanced (Maquet et al., 1996), they conceive of REMS as a program for exploring weak, novel cortical associations and evaluating them in light of emotional input from the limbic system. This theory is compatible with another from Jouvet, in which ponto-geniculo-occipital waves from the brainstem stimulate a gene-mediated reprogramming of the dreaming brain, one which integrates cortical and genetic influences, and which is encoded by the hippocampal theta rhythm, allowing genetic control of psychological variability post-neurogenesis (Jouvet, 1998). Also compatible is the theory put forward by Llewellyn and Hobson (2015), proposing that REMS creates spatial and associative maps of emotionally salient landmarks through an exploratory “pre-play”. In all of these theories, REMS brings out weak links that, while less correlated with the environment, hold the possibility of high adaptive returns, be they mapmaking, creative problem solving or genetic control of psychological variation. Inevitably, the reinforcement of weaker links entails the relative depreciation of stronger ones. Existing connections drawn from experience may be weakened as a result. Hence, REMS and its neural mechanisms, such as theta-gamma PAC, may be

detrimental to declarative memory consolidation, in favour of cortical exploration. In contrast, NREMS and its distilling oscillatory mechanisms may eliminate weak links in favour of the strong ones. In this way, REMS and NREMS would be analogous to the see-sawing opposition between exploration and exploitation, respectively (see Cohen et al., 2007; Hills et al., 2015). The exploration-exploitation trade-off (or the the stability-flexibility trade-off) is a problem encountered in domains as varied as decision-making (Cohen et al., 2007), visual search (Wolfe et al., 1989), fungal growth (Watkinson et al., 2005), and machine learning (Kaelbling et al., 1996). Briefly, it asks how much of a limited resource (usually time) should be devoted to exploiting known strategies, and how much should be devoted to exploring new, uncertain strategies that may be more or less beneficial. The answer is nontrivial and usually involves a bit of both (Cohen et al., 2007). In sleep, the limited resource at play may be memory, which we may operationalize as the excitability of neural circuits. NREMS may devote memory (i.e. excitability) to exploiting known information by stabilizing and abstracting daytime learning, while REMS may sacrifice the stability of this information by diverting memory to stochastically explored patterns of unknown (and potentially higher) value.

In discussing the human REMS theta rhythm, we have not addressed its source. In animal studies, invasive techniques allow the reliable recording of a strong tonic hippocampal theta rhythm in REMS (Montgomery et al., 2008; Scheffzük et al., 2011). In humans, ethical considerations limit the invasive recording of subcortical structures to cases of intractable epilepsy, so studies are few. Those that have recorded in the vicinity of the human hippocampus during REMS have either found a weak phasic (~ 1s) theta (Cantero et al., 2003) or a strong, tonic delta (Bódizs et al., 2001; Clemens et al., 2009). The latter finding, in conjunction with the finding that the wavelength and the volumetric extent of an oscillation in the brain are correlated (von Stein and Sarnthein, 2000), suggests that the hippocampal theta of ancestral mammals has slowed in the course of human evolution, in step with increasing brain size (Bódizs et al., 2001; Buzsáki et al., 2013; Jacobs, 2014). In addition, it is unclear whether an oscillation in the human hippocampus can be detected at the scalp, and to complicate matters, there is evidence of human neocortical theta sources (Kahana et al., 2001; Mitchell et al., 2008). Notably, frontal midline theta recorded from the human scalp is associated with mnemonic and attentional function, similar to hippocampal theta in rats. Notwithstanding these caveats, since the hippocampus has widespread monosynaptic connections to the neocortex, and since scalp EEG mostly detects the post-synaptic potentials of pyramidal neurons in the neocortex, and assuming that low-frequency oscillations represent rhythmic volleys of postsynaptic excitation and inhibition, it is possible that weak hippocampal oscillations can be indirectly measured on the

human scalp from their postsynaptic effects on pyramidal neurons. If this is the case, the low-frequency phase-giving oscillations underlying the theta-gamma and delta-gamma PAC detected in the present study could be the human homologue of hippocampal theta in non-human animals. If not, these rhythms are then possibly of neocortical origin, although precise localization of scalp EEG sources is complicated by the inverse problem (Koles, 1998; Mitchell et al., 2008). The fact that we could not detect REMS PAC using power-triggered MI analysis argues in favour of a low-power phase-giving rhythm at work. Furthermore, a learning-related hippocampal theta-gamma PAC has been demonstrated in waking studies of humans using intracranial EEG (Axmacher et al., 2010) and magnetoencephalography (Poch et al., 2010). We may then envision delta/theta-gamma PAC as a mechanism for projecting neuronal activity into space and time, with hippocampal theta/delta organizing neocortical gamma by its phase, moulding it into a form that is available for recall as spatiotemporal, or episodic, memory—a system which has been co-opted in humans for building a cognitive, associational space (Buzsáki and Moser, 2014).

Nowhere did we detect a relationship between pre-sleep successful recall and subsequent sleep CFC or oscillatory parameters (Model 3). Considered in juxtaposition with effects of the learning task on CFC, this finding indicates that it is not successful recall-enabling encoding, but exposure to a learning opportunity, which modulates sleep CFC. It may be that participants encoded a similar number of declarative memories during the task, but that other factors, such as competing cortical activation, affected their ability to recall pre-sleep. Later, sleep CFC undertook the integration and consolidation of these memories, modulating their “recallability” on the post-sleep test.

A complicating aspect of our results is that learning effects on PAC were detected at Cz, whereas our strongest predictions of recall came from PAC at Fz. It should be noted that we applied the comodulogram analysis only to Cz; therefore, it may be that an Fz comodulogram would reveal a learning-related increase corresponding to the predictive PAC. Another inconsistency is that we detected a learning-related delta-sigma PAC increase at Cz with *a priori* bands, but not with the comodulogram. The explanation may lie in the lower limit of the comodulogram set at 0.83 Hz (adapted frequency), whereas the lower limit of the *a priori* delta band was 0.25 Hz; thus, the strongest PAC increase may have been at phase band 0.25-0.83 Hz. Also, the analysis epochs were much longer in the comodulogram (several minutes) than in the *a priori* analysis (30 s), so that the analyses are detecting different scales of PAC. It may be that the phase of delta-sigma PAC is less consistent in longer durations. However, the coupling phase analysis seems to show a consistency (Fig. 16). Lastly, the comodulogram used delta

adapted bands, extrapolated from individual sigma peaks. It may be that this individual adjustment is not suitable for delta waves.

### *Limitations*

Some methodological limitations of this study warrant mention. Firstly, the limited size of our participant sample (n=10) may have resulted in underpowered analyses. Next, as mentioned just previously, our more stringent power-triggered MI analysis was ineffective. This either means that there was in fact no effect to be found, or the power-triggered MI analysis is inadequate for detecting the effect. Aru et al. (2015) state that PAC is meaningless without a concomitant power rise in the phase-giving frequency. In our data, we detected spectral peaks in both NREMS delta and REMS theta at the minutes scale, but were unable to show seconds-scale rises in power concomitant with learning-related PAC changes. This may be explained by the choice of analysis epochs for power-triggered analysis. Whereas in the *a priori* analysis we applied the MI to 30-s epochs and then averaged, in the power-triggered analysis, we instead concatenated all relevant signal before applying the MI, resulting in a signal several minutes long. This was necessary, because the snippets of power-triggered signal were too short for reliable PAC detection (Tort et al., 2010). However, the concatenation of non-consecutive sections of signal introduced artificial non-stationarities, which may have biased the MI (Aru et al., 2015). Moreover, the MI underestimates PAC if there are fluctuations in coupling phase throughout the signal, and this risk escalates with prolonged signal duration. This last caveat is less an issue than it is a qualification of our PAC data: what we have measured is the consistent biasing, to a certain coupling phase or phases, of amplitude variations in one signal by the phase of another, on the scale of minutes and not seconds. The same concatenation method was used in the comodulogram analysis, but for all signal for the relevant stage, creating even longer signals (tens of minutes). Differences in MI analysis epochs may thus explain discrepancies between the *a priori*, power-triggered and comodulogram analyses, which are measuring small (30 s), medium (>1 min) and large-scale (>10 min) PAC, respectively.

Next, the comodulogram analysis presented some issues. First, as mentioned previously, the dynamic bandwidth employed for the amplitude frequency axis afforded progressively sparser coverage as the amplitude- to phase-frequency ratio increased. Since PAC has often been detected in low-to-high frequency ranges (Clemens et al., 2009; Amiri et al., 2016), this feature of the comodulogram was perhaps ill-suited. On the other hand, the dynamic bandwidth had the advantage of controlling for changes in phase-frequency-to-amplitude-bandwidth ratio that could bias PAC magnitude (Aru et al., 2015). Still, an improved comodulogram could impose

a lower limit on the dynamic amplitude band, to ensure that all amplitude frequencies are captured for each phase frequency band. The sparseness in the present comodulogram may explain why the effect of learning on delta-sigma PAC detected using *a priori* bands was not replicated in the comodulogram.

Previous studies employing the MI for PAC detection often used surrogate data comparisons to determine the statistical significance of PAC (Tort et al., 2010). Since we were interested in PAC differences and correlations, we did not deem this procedure necessary. Because of this, we cannot ascertain that the PAC values we report are greater than what may have arisen from the signal by chance. Also, we cannot determine whether a detected PAC difference is due to increased synchronization in one condition or desynchronization in the other. Likewise, for PAC correlations, we cannot determine whether variation is due to magnitude changes or quantum changes in the presence of statistically significant PAC.

Lastly, we evaluated oscillatory parameters by averaging over all sleep cycles, whereas our findings for NREMS PAC were in the first cycle only. A more faithful comparison of the influences of PAC and oscillatory parameters would take all measurements from the same period.

### *Next steps*

We are now working to complement these analyses. Four more participants have been recorded and will be added to the sample for all analyses. In addition to implementing improvements in the method that were proposed in the previous section, we will extend our comodulogram analysis to Fz, to determine whether PAC correlations with learning at this derivation are accompanied by learning-related increases. Further, we will correlate learning-related changes in PAC from the comodulograms *ad hoc* with memory performance. It will be interesting to test the prediction that theta-gamma PAC in NREMS is negatively correlated with declarative memory performance. In addition, we will extend our analyses to other scalp derivations. Finally, we will perform additional analyses matching those of Gais et al. (2002), Schabus et al. (2004), Fogel et al. (2007), Mölle et al. (2009), Cox et al. (2012) and Niknazar et al. (2015), in order to better replicate their studies.

### *Concluding remarks*

We have provided strong support for the prediction that the temporal organization of SWs and spindles reflects effective sleep-dependent consolidation of declarative memories (Staresina et al., 2015). Furthermore, we have demonstrated a novel, detrimental effect of REMS theta-

gamma PAC on declarative memory consolidation, one which may illuminate the elusive role of this paradoxical sleep stage. While NREMS may integrate new memories from waking activity into prior knowledge networks and make them available for recall, REMS may instead recombine these memories in creative and adaptive ways, at the cost of recall efficiency. To put it in familiar terms, if life is a research project, waking is data collection, NREMS is analysis, and REMS is speculation (with the occasional emotional bias). The two states of mammalian sleep may operate as opponent processes, nightly striving for the optimum between cortical exploration and exploitation (see Cohen et al., 2007; Hills et al., 2015).

The adaptive benefit of REMS may have dwindled in humans as a result of the rapid expansion of the neocortex and its creative prowess, so that this vigilance state may now be a mere vestige; indeed, it is not missed when abolished by antidepressants or other drugs (Vogel et al., 1990). Incidentally, in light of the preceding discussion, it may be worthwhile to examine whether the benefit of REMS deprivation for ameliorating depression is due to an abolishment of theta-gamma PAC-mediated memory formation during REMS. It may be that in some forms of major depression, negative emotionality of cortical (Wagner et al., 2001; Nishida et al., 2009) or genetic origin (Jouvet, 1998) invades the brain in REMS and through theta-mediated encoding, primes the waking brain for depression, in a vicious cycle. Cannabis has been shown to disrupt hippocampal theta and theta-gamma PAC in the hippocampus (Robbe et al., 2006; Robbe and Buzsáki, 2009), and could assist in an informative test of this hypothesis.

To reiterate, electrical activity is segregated in space and time in the mammalian brain. From the foregoing discussion, we may posit that temporal segregation in fact encodes both space and time. Awake, and perhaps during REMS, perceptions and emotions are at once parsed into moments and situated along spatiotemporal dimensions by a slow hippocampal rhythm. Asleep, NREMS spontaneous activity relives these moments one at a time through the lens of knowledge, enveloping them in a hierarchy of waves to preserve the partition of where and when.

## References

Amiri M, Frauscher B, Gotman J (2016) Phase-amplitude coupling is elevated in deep sleep and in the onset zone of focal epileptic seizures. *Front Hum Neurosci* 10:1-12.

Aru J, Aru J, Priesemann V, Wibral M, Lana L, Pipa G, Singer W, Vicente R (2015) Untangling cross-frequency coupling in neuroscience. *Curr Opin Neurobiol* 31:51-61.

Axmacher N, Elger CE, Fell J (2008) Ripples in the medial temporal lobe are relevant for human memory consolidation. *Brain* 131:1806-1817.

Axmacher N, Henseler MM, Jensen O, Weinreich I, Elger CE, Fell J (2010) Cross-frequency coupling supports multi-item working memory in the human hippocampus. *PNAS* 107:3228-3233.

Ayoub A, Mölle M, Preissl H, Born J (2012) Grouping of MEG gamma oscillations by EEG sleep spindles. *Neuroimage* 59:1491-1500.

Bódizs R, Kántor S, Szabó G, Szûcs A, Eröss L, Halász P (2001) Rhythmic hippocampal slow oscillation characterizes REM sleep in humans. *Hippocampus* 11:747-753.

Boyce R, Glasgow SD, Williams S, Adamantidis A (2016) Causal evidence for the role of REM sleep theta rhythm in contextual memory consolidation. *Science* 352:812-816.

Brankač J, Scheffzük C, Kukushka VI, Vyssotski AI, Tort ABL, Draguhn A (2012) Distinct features of fast oscillations in phasic and tonic rapid eye movement sleep. *J Sleep Res* 21:630-633.

Buzsáki G (1989) Two-stage model of memory trace formation: A role for "noisy" brain states. *Neuroscience* 31:551-570.

Buzsáki G (1996) The hippocampo-neocortical dialogue. *Cereb Cortex* 6:81-92.

Buzsáki G (2006) *Rhythms of the Brain*. New York: Oxford UP.

Buzsáki G (2010) Neural syntax: cell assemblies, synapsembles and readers. *Neuron* 68:362-385.

Buzsáki G, Draguhn A (2004) Neuronal oscillations in cortical networks. *Science* 304:1926-1929.

Buzsáki G, Logothetis N, Singer W (2013) Scaling brain size, keeping time: Evolutionary preservation of brain rhythms. *Neuron* 80:751-764.

Buzsáki G, Mizuseki K (2014) The log-dynamic brain: how skewed distributions affect network operations. *Nat Rev Neurosci* 15:264-278.

Buzsáki G, Moser E (2014) Memory, navigation and theta-rhythm in the hippocampal-entorhinal system. *Nat Neurosci* 16:130-138.

Canolty RT, Edwards E, Dalal SS, Soltani M, Nagarajan SS, Kirsch HE, Berger MS, Barbaro NM, Knight RT (2006) High gamma power is phase-locked to theta oscillations in human neocortex. *Science* 313: 1626-1628.

Canolty RT, Knight RT (2010) The functional role of cross-frequency coupling. *Trends Cogn Sci* 14:506-515.

Cantero JL, Atienza M, Stickgold R, Kahana MJ, Madsen JR, Kocsis B (2003) Sleep-dependent  $\theta$  oscillations in the human hippocampus and neocortex. *J Neurosci* 23:10897-10903.

Clemens Z, Mölle M, Eröss L, Barsi P, Halász P, Born J (2007) Temporal coupling of parahippocampal ripples, sleep spindles and slow oscillations in humans. *Brain* 130:2868-2878.

Clemens Z, Weiss B, Szűcs A, Eröss L, Rásonyi G, Halász P (2009) Phase coupling between rhythmic slow activity and gamma characterizes mesiotemporal rapid-eye-movement sleep in humans. *Neuroscience* 163:388-396.

Cohen J, McClure SM, Yu AJ (2007) Should I stay or should I go? How the human brain manages the trade-off between exploitation and exploration. *Philos Trans R Soc Lond B: Biol Sci* 362:933-942.

- Contreras D, Steriade M (1995) Cellular basis of EEG slow rhythms: A study of dynamic corticothalamic relationships. *J Neurosci* 15:604-622.
- Contreras D, Steriade M (1996) Spindle oscillations in cats: the role of corticothalamic feedback in a thalamically generated rhythm. *J Physiol* 490:159-179.
- Cox R, Hofman WF, Talamini LM (2012) Involvement of spindles in memory consolidation is slow wave sleep-specific. *Learn Memory* 19:264–267.
- Diekelmann S, Born J (2010) The memory function of sleep. *Nature* 467:114-126.
- Engel AK, Gerloff C, Hülsmann J, Nolte G (2013) Intrinsic of coupling modes: Multiscale interactions in ongoing brain activity. *Neuron* 80:867-886.
- Eschenko O, Ramadan W, Mölle M, Born J, Sara SJ (2008) Sustained increase in hippocampal sharp-wave ripple activity during slow-wave sleep after learning. *Learn Memory* 15:222-228.
- Fell J, Fernández G, Lutz MT, Kockelman E, Burr W, Schaller C, Elger CE, Helmstaedter C (2006) Rhinal-hippocampal connectivity determines memory formation during sleep. *Brain* 129:108-114.
- Finelli LA, Achermann P, Borbély AA (2001) Individual ‘fingerprints’ in human sleep EEG topography. *Nature* 412:S57-S62.
- Fogel SM, Smith CT, Cote KA (2007) Dissociable learning-dependent changes in REM and non-REM sleep in declarative and procedural memory systems. *Behav Brain Res* 180:48–61.
- Fries P (2005) A mechanism for cognitive dynamics: neuronal communication through neuronal coherence. *Trends Cogn Sci* 9:474-480.
- Gais S, Mölle M, Helms K, Born J (2002) Learning-dependent increases in sleep spindle density. *J Neurosci* 22:6830-6834.

Girardeau G, Benchenane K, Wiener SI, Buzsáki G, Zugaro MB (2009) Selective suppression of hippocampal ripples impairs spatial memory. *Nat Neurosci* 12:1222-1223.

Gupta AS, van der Meer MAA, Touretzky DS, Redish AD (2010) Hippocampal replay is not a simple function of experience. *Neuron* 65:695-705.

Hasenstaub A, Shu Y, Haider B, Kraushaar U, Duque A, McCormick DA (2005) Inhibitory postsynaptic potentials carry synchronized frequency information in active cortical networks. *Neuron* 47:423-435.

Hills TT, Todd PM, Lazer D, Redish AD, Couzin ID, the Cognitive Search Research Group (2015) Exploration versus exploitation in space, mind and society. *Trends Cogn Sci* 19:46-54.

Huber R, Ghilardi F, Massimini M, Tononi G (2004). Local sleep and learning. *Nature* 430:78-81.

Iber C, Ancoli-Israel S, Chesson AL, Quan SF (2007) The AASM manual for the scoring of sleep and associated events. Westchester, IL: American Academy of Sleep Medicine.

Isomura Y, Sirota A, Özen S, Montgomery S, Mizuseki K, Henze DA, Buzsáki G (2006) Integration and segregation of activity in entorhinal-hippocampal subregions by neocortical slow oscillations. *Neuron* 52:871-882.

Jacobs J (2014) Hippocampal theta oscillations are slower in humans than in rodents: implications for models of spatial navigation and memory. *Philos T R Soc B* 369: 1-9.

Jacobs J, Kahana MJ, Ekstrom AD, Fried I (2007) Brain oscillations control timing of single neuron activity in humans. *J Neurosci* 27:3839-3844.

Jensen O (2006) Maintenance of multiple working memory items by temporal segmentation. *Neuroscience* 139:237-249.

Jensen O, Colgin LL (2007) Cross-frequency coupling between neuronal oscillations. *Trends Cogn Sci* 11:267-269.

Jouvet M (1998) Paradoxical sleep as a programming system. *J Sleep Res* 7:1-5.

Kaelbling LP, Littman ML, Moore AW (1996) Reinforcement learning: a survey. *J Artif Intell Res* 4:237-285.

Kahana MJ, Seelig D, Madsen JR (2001) Theta returns. *Curr Op Neurobiol* 11:739-744.

Kaplan R, Bush D, Bonnefond M, Bandettini PA, Barnes GR, Doeller CF, Burgess N (2014) Medial prefrontal theta phase coupling during spatial memory retrieval. *Hippocampus* 24:656-665.

Klinzing JG, Mölle M, Weber F, Supp G, Hipp JF, Engel AK, Born J (2016) Spindle activity phase-locked to sleep slow oscillations. *Neuroimage* 134:607-616.

Koles ZJ (1998) Trends in EEG source localization. *EEG Clin Neurophysiol* 196:127-137.

Lega B, Burke J, Jacobs J, Kahana MJ (2014) Slow-theta-to-gamma phase-amplitude coupling in hippocampus supports the formation of new episodic memories. *Cereb Cortex*: bhu232.

Leopold DA, Murayama Y, Logothetis NK (2003) Very slow activity fluctuations in monkey visual cortex: Implications for functional brain imaging. *Cereb Cortex* 13:422-433.

Lewis PA, Durrant SJ (2011) Overlapping memory replay during sleep builds cognitive schema. *Trends in Cogn Sci* 15:343-351.

Llewellyn S, Hobson JA (2015) Not only... but also: REM sleep creates and NREM stage 2 instantiates landmark junctions in cortical memory networks. *Neurobiol Learn Mem* 122:69-87.

Maquet P, Péters JM, Aerts J, Delfiore G, Degueldre C, Luxen A, Franck G (1996) Functional neuroanatomy of human rapid-eye-movement sleep and dreaming. *Nature* 383:163-166.

Marshall L, Helgadóttir H, Mölle M, Born J (2006) Boosting slow oscillations during sleep potentiates memory. *Nature* 444:610-613.

Marshall L, Kirov R, Brade J, Mölle M, Born J (2011) Transcranial electrical currents to probe EEG brain rhythms and memory consolidation during sleep in humans. *Plos One* 6:1-10.

Mednick SC, McDevitt EA, Walsh JK, Wamsley E, Paulus M, Kanady JC, Drummond SPA (2013) The critical role of sleep spindles in hippocampal-dependent memory: a pharmacology study. *J Neurosci* 33:4494-4504.

Mitchell DJ, McNaughton N, Flanagan D, Kirk IJ (2008) Frontal-midline theta from the perspective of hippocampal “theta”. *Prog Neurobiol* 86:156-185.

Mölle M, Bergmann TO, Marshall L, Born J (2011) Fast and slow spindles during the sleep slow oscillation: Disparate coalescence and engagement in memory processing. *Sleep* 34:1411-1421D.

Mölle M, Eschenko O, Gais S, Sara SJ, Born J (2009) The influence of learning on sleep slow oscillations and associated spindles and ripples in humans and rats. *Eur J Neurosci* 29:1071-1081.

Mölle M, Marshall L, Gais S, Born J (2002) Grouping of spindle activity during slow oscillations in human non-rapid eye movement sleep. *J Neurosci* 22:10941-10947.

Montgomery SM, Sirota A, Buzsáki G (2008) Theta and gamma coordination of hippocampal networks during waking and REM sleep. *J Neurosci* 28:6731-6741.

Moroni F, Nobili L, Curcio G, De Carli F, Tempesta D, Marzano C, De Gennaro L, Mai R, Francione S, Lo Russo G, Ferrara G (2008) Procedural learning and sleep hippocampal low frequencies in humans. *Neuroimage* 42:911-918.

Nere A, Hashmi A, Cirelli C, Tononi G (2013) Sleep-dependent synaptic down-selection (I): modeling the benefits of sleep on memory consolidation and integration. *Front Neurol* 4:1-17.

New B, Pallier C, Ferrand L, Matos R (2001) Une base de données lexicales du français contemporain sur internet: LEXIQUE. *Ann Psychol* 101:447-462.

Ngo HVV, Martinetz T, Born J, Mölle M (2013) Auditory closed-loop stimulation of the sleep slow oscillation enhances memory. *Neuron* 78:545-553.

Niknazar M, Krishnan GP, Bazhenov M, Mednick SC (2015) Coupling of thalamocortical sleep oscillations are important for memory consolidation in humans. *Plos One* 10:e1044720.

Nishida M, Pearsall J, Buckner RL, Walker MP (2009) REM sleep, prefrontal theta, and the consolidation of human emotional memory. *Cereb Cortex* 19:1158–1166.

Nunez, PL (1981) *Electric fields of the brain*. New York: Oxford UP.

O'Keefe J, Recce ML (1993) Phase relationship between hippocampal place units and the EEG theta rhythm. *Hippocampus* 3:317-330.

Osipova D, Takashima A, Oostenveld R, Fernández G, Maris E, Jensen O (2008) Theta and gamma oscillations predict encoding and retrieval of declarative memory. *J Neurosci* 26:7523-7531.

Peyrache A, Battaglia FP, Destexhe A (2011) Inhibition recruitment in prefrontal cortex during sleep spindles and gating of hippocampal inputs. *PNAS* 108:17207-17212.

Piantoni G, Astill RG, Raymann RJEM, Vis JC, Coppens JE, Van Someren EJW (2013) Modulation of gamma and spindle-range power by slow oscillations in scalp sleep EEG of children. *Int J Psychophysiol* 89:252-258.

Plihal W, Born J (1997) Effects of early and late nocturnal sleep on declarative and procedural memory. *J Cogn Neurosci* 9:534-547.

Poch C, Fuentemilla L, Barnes GR, Düzel E (2010) Hippocampal theta-phase modulation of replay correlates with configural-relational short-term memory performance. *J Neurosci* 31:7038-7042.

Poe GR, Walsh CM, Bjorness TE (2010) Cognitive neuroscience of sleep. *Prog Brain Res* 185:1-19.

Rasch B, Born J (2013) About sleep's role in memory. *Physiol Rev* 93:681-766.

Robbe D, Buzsáki G (2009) Alteration of theta timescale dynamics of hippocampal place cells by a cannabinoid is associated with memory impairment. *J Neurosci* 29:12597-12605.

Robbe D, Montgomery SM, Thome A, Rueda-Orozco PE, McNaughton BL, Buzsáki G (2006) Cannabinoids reveal the importance of spike timing coordination in hippocampal function. *Nat Neurosci* 9:1526-1533.

Sauseng P, Klimesch W, Heise KF, Gruber WR, Holz E, Karim AA, Glennon M, Gerloff C, Birbaumer N, Hummel FC (2009) Brain oscillatory substrates of visual short-term memory capacity. *Curr Biol* 19:1846-1852.

Schabus M, Gruber G, Parapatics S, Sauter C, Klösch G, Anderer P, Klimesch W, Saletu B, Zeitlhofer J (2004) Sleep spindles and their significance for declarative memory consolidation. *Sleep* 27:1479-1485.

Scheffer-Teixeira R, Belchior H, Caixeta FV, Souza BC, Ribeiro S, Tort ABL (2011) Theta phase modulates multiple layer-specific oscillations in the CA1 region. *Cereb Cortex* 22:2404-2414.

Scheffzük C, Kukushka VI, Vyssotski AL, Draguhn A, Tort ABL, Brankač J (2011) Selective coupling between theta phase and neocortical fast gamma oscillations during REM-sleep in mice. *Plos One* 6:1-9.

Shirvalkar PR, Rapp PR, Shapiro ML (2009) Bidirectional changes to hippocampal theta-gamma comodulation predict memory for recent spatial episodes. *PNAS* 107:7054-7059.

Siegel JM (2001) The REM sleep-memory consolidation hypothesis. *Science* 294:1058-1063.

Siegel JM (2005) Clues to the function of mammalian sleep. *Nature* 437:1264-1271.

Sirota A, Csicsvari J, Buhl D, Buzsáki G (2003) Communication between neocortex and hippocampus during sleep in rodents. *PNAS* 100:2065-2069.

Soltesz I, Deschênes M (1993) Low- and high-frequency membrane potential oscillations during theta activity in CA1 and CA3 pyramidal neurons of the rat hippocampus under ketamine-xylazine anesthesia. *J Neurophysiol* 70:97-116.

Staresina BP, Bergmann TO, Bonnefond M, van der Meij R, Jensen O, Deuker L, Elger CE, Axmacher N, Fell J (2015) Hierarchical nesting of slow oscillations, spindles and ripples in the human hippocampus during sleep. *Nat Neurosci* 18:1679–1686.

Staudigl T, Hanslmayr S (2013) Theta oscillations at encoding mediate the context-dependent nature of human episodic memory. *Curr Biol* 23:1101-1106.

Steriade, M (2006) Grouping of brain rhythms in corticothalamic systems. *Neuroscience* 137:1087-1106.

Steriade M, McCormick DA, Sejnowski TJ (1993) Thalamocortical oscillations in the sleeping and aroused brain. *Science* 262:679-685.

Stickgold R, Hobson JA, Fosse R, Fosse M (2001) Sleep, learning, and dreams: off-line memory reprocessing. *Science* 294:1052-1057.

Stickgold R, Walker MP (2013) Sleep-dependent memory triage: evolving generalization through selective processing. *Nature Neurosci* 16:139-145.

Sweeney-Reed CM, Zaehle T, Voges J, Schmitt FC, Buentjen L, Kopitzki K, Esslinger C, Hinrichs H, Heinze HJ, Knight RT, Richardson-Klavehn A (2014) Corticothalamic phase synchrony and cross-frequency coupling predict human memory formation. *Elife* 3:e05352.

Takeuchi S, Murai R, Shimazu H, Isomura Y, Mima T, Tsujimoto T (2016) Spatiotemporal organization and cross-frequency coupling of sleep spindles in primate cerebral cortex. *Sleep* 39:1719-1735.

Tinguely G, Finelli LA, Landolt HP, Borbély AA, Achermann P (2006) Functional EEG topography in sleep and waking: state-dependent and state-independent features. *Neuroimage* 32:283-292.

Tort ABL, Komorowski R, Eichenbaum H, Kopell N (2010) Measuring phase-amplitude coupling between neuronal oscillations of different frequencies. *J Neurophysiol* 104:1195-1210.

Tort ABL, Komorowski R, Manns JR, Kopell N, Eichenbaum H (2009) Theta-gamma coupling increases during the learning of item-context associations. *PNAS* 106:20942-20947.

Tononi G, Cirelli C (2006) Sleep function and synaptic homeostasis. *Sleep Med Rev* 10:49-62.

Tononi G, Cirelli C (2014) Sleep and the price of plasticity: from synaptic and cellular homeostasis to memory consolidation and integration. *Neuron* 81:12-34.

Tononi G, Sporns O, Edelman G (1996) A complexity measure for selective matching of signals by the brain. *PNAS* 93:3422-3427.

Varela F, Lachaux JP, Rodriguez E, Martinerie J (2001) The brain web: phase synchronization and large-scale integration. *Nat Rev Neurosci* 2:229-239.

Vertes RP (2004) Memory consolidation in sleep: Dream or reality. *Neuron* 44:135-148.

Vogel GW, Buffenstein A, Minter K, Hennessey A (1990) Drug effects on REM sleep and on endogenous depression. *Neurosci Biobeh Rev* 14:49-63.

von Stein A, Sarnthein J (2000) Different frequencies for different scales of cortical integration: from local gamma to long range alpha theta synchronization. *Intl J Psychophysiol* 38:301-313.

Wagner U, Gais S, Born J (2001) Emotional memory formation is enhanced across sleep intervals with high amounts of rapid eye movement sleep. *Learn Memory* 8:112-119.

Walker MP, Stickgold R (2004) Sleep-dependent learning and memory consolidation. *Neuron* 44:121-133.

Watkinson SC, Boddy L, Burton K, Darrah PR, Eastwood D, Fricker MD, Tlalka M (2005) New approaches to investigating the function of mycelial networks. *Mycologist* 19:11-17.

Wilson MA, McNaughton BL (1994) Reactivation of hippocampal ensemble memories during sleep. *Science* 265:676-679.

Wolfe JM, Cave KR, Franzel SL (1989) Guided search: an alternative to the feature integration model for visual search. *J Exp Psychol Hum Percept Perform* 15:419-433.

Zerouali Y, Lina JM, Sekerovic Z, Godbout J, Dubé J, Jolicoeur P, Carrier J (2014) A time-frequency analysis of the dynamics of cortical networks of sleep spindles from MEG-EEG recordings. *Front Neurosci* 8:1-13.

## Tables

Table 1

*Participant characteristics (N = 10)*

<b>Characteristics</b>	<b>Mean (SD)</b>	<b>Range</b>
Age	23.3 (3.2)	19-30
Years of education	15.9 (2.0)	12-18
CES-D	7.1 (4.8)	1-15
PSQI	2.8 (1.3)	1-4
MEQ-SA	53.4 (8.5)	38-68
ESS	4.8 (2.1)	2-7
ISI	3.4 (2.2)	0-6
BDI	1.8 (2.3)	0-5
BAI	2.0 (4.1)	0-13
EHI	0.66 (0.27)	0.33-1.00

*Note.* BAI, Beck anxiety inventory; BDI, Beck's depression inventory; CES-D, Centre for Epidemiological Studies – Depression screening; EHI, Edinburgh handedness inventory; ESS, Epworth sleepiness scale; ISI, insomnia severity index; MEQ-SA, morningness-eveningness questionnaire – self-assessment version; PSQI, Pittsburgh sleep quality index.

Table 2

*Sleep parameters on experimental nights (N = 10)*

<b>Parameters</b>	<b>Control, M (SD)</b>	<b>Learning, M (SD)</b>	<b>F</b>	<b>P</b>
Total sleep time (min)	379.00 (91.29)	393.00 (65.10)	0.62	0.81
WASO (min)	14.25 (12.82)	21.20 (37.44)	1.14	0.32
Sleep onset latency (min)	7.35 (9.01)	19.30 (30.41)	0.24	0.64
Sleep efficiency (%)	93.72 (3.87)	88.80 (9.96)	0.11	0.75
Stage N1 (% of TST)	3.63 (2.11)	3.97 (4.23)	0.23	0.65
Stage N2 (% of TST)	44.12 (8.04)	43.23 (10.59)	0.59	0.47
Stage N3 (% of TST)	28.27 (10.77)	29.87 (11.07)	0.05	0.83
Stage REMS (% of TST)	23.90 (5.82)	22.25 (4.51)	0.33	0.58
1 <sup>st</sup> NREMS period (min)	79.00 (24.73)	68.25 (13.33)	2.55	0.15

*Note.* *F*-statistic and *p*-value are for main effect in ANCOVA with control and learning nights as repeated measures and age as covariate. TST, total sleep time WASO, wake after sleep onset;.

Table 3

*Learning task performance by participant*

<b>Participant</b>	<b>Pre-sleep score (%)</b>	<b>Post-sleep score (%)</b>	<b>Change (% of total)</b>
1	50 (41.7)	47 (39.2)	-3 (-2.5)
2	55 (45.8)	55 (45.8)	0 (0)
3	38 (31.7)	32 (26.7)	-6 (-5.0)
4	35 (29.2)	36 (30.0)	1 (0.83)
5	87 (72.5)	90 (75.0)	3 (2.5)
6	115 (95.8)	116 (96.7)	1 (0.83)
7	49 (40.8)	50 (41.7)	1 (0.83)
8	100 (83.3)	100 (83.3)	0 (0)
9	9 (7.5)	10 (8.3)	1 (0.83)
10	47 (39.2)	43 (35.8)	-4 (-3.3)
Mean	59.8 (49.8)	59.6 (49.6)	-0.22 (-0.19)

*Note.* The absolute number of word pairs recalled are shown, with percentages out of the total of 120 word pairs indicated in parentheses.

Table 4

Comparison of NREMS oscillatory parameters on experimental nights ( $N = 10$ )

Parameters	Fz				Cz			
	Control M (SD)	Learning M (SD)	F	P	Control M (SD)	Learning M (SD)	F	P
<b>Slow wave</b>								
Density	1.89 (1.51)	1.84 (1.29)	0.001	1.00	1.18 (0.92)	1.45 (0.86)	3.15	0.11
Duration (s)	1.25 (0.18)	1.26 (0.24)	1.16	0.31	1.28 (0.24)	1.31 (0.25)	0.99	0.35
RMS ( $\mu$ V)	66.70 (6.61)	68.07 (7.93)	5.37	0.049*	64.10 (5.85)	65.93 <sup>†</sup> (7.17)	2.57	0.15
Amplitude ( $\mu$ V)	200 (17.6)	201 (19.7)	5.29	0.050	194 (14.8)	197 <sup>†</sup> (15.6)	0.99	0.35
Delta power, normalized (%)	85.94 (3.19)	85.34 (4.15)	1.57	0.25	82.95 (3.91)	83.68 (3.99)	1.39	0.27
<b>Spindle</b>								
Density	1.47 (0.21)	1.45 (0.26)	0.008	0.93	1.69 (0.18)	1.65 (0.27)	0.74	0.41
Duration (s)	0.80 (0.03)	0.81 (0.05)	1.51	0.25	0.81 (0.04)	0.82 (0.05)	0.14	0.72
RMS ( $\mu$ V)	8.65 (2.38)	8.46 (2.88)	1.33	0.28	9.49 (2.88)	8.68 (2.76)	1.27	0.29
Sigma power, normalized (%)	1.04 (0.68)	1.10 (0.94)	1.02	0.34	1.43 (0.85)	1.18 (0.84)	3.41	0.10

*Note.*  $F$ -statistic and  $p$ -value are for the main effect in ANCOVA with control and learning nights as repeated measures and age as covariate. Spindle and SW parameters are for all N2 and N3 epochs. M, mean; RMS, root-mean-square; SD, standard deviation. \* $p < 0.05$

Table 5

Comparison of REMS oscillatory parameters on experimental nights ( $N = 10$ )

Parameters	Fz				Cz			
	Control M (SD)	Learning M (SD)	F	P	Control M (SD)	Learning M (SD)	F	P
<b>Delta train</b>								
Density	2.51 (0.78)	2.79 (0.39)	1.68	0.23	2.73 (0.79)	2.90 (0.34)	0.97	0.36
Duration (s)	0.91 (0.08)	0.87 (0.03)	2.14	0.18	0.92 (0.09)	0.89 (0.04)	1.37	0.28
RMS ( $\mu$ V)	28.44 (12.71)	25.15 (8.12)	0.16	0.70	29.88 (11.41)	28.76 (12.83)	0.12	0.92
Delta power, normalized (%)	19.57 (4.47)	18.08 (4.90)	2.95	0.12	21.23 (5.85)	18.01 (6.10)	5.39	0.049
<b>Theta train</b>								
Density	1.56 (0.28)	1.73 (0.23)	0.94	0.36	1.68 (0.21)	1.75 (0.26)	0.04	0.84
Duration (s)	0.82 (0.06)	0.82 <sup>†</sup> (0.07)	0.24	0.64	0.81 (0.04)	0.80 (0.04)	2.39	0.16
RMS ( $\mu$ V)	35.71 (20.61)	31.29 (10.17)	0.10	0.76	37.20 (16.76)	35.29 (12.34)	<0.001	1.00
Theta power, normalized (%)	10.48 (3.63)	9.95 (4.08)	2.19	0.18	13.04 (5.99)	11.54 (6.89)	1.23	0.30
Gamma power, normalized (%)	2.89 (2.36)	1.81 (1.13)	0.04	0.85	3.16 (2.38)	1.84 (1.03)	0.24	0.64

Note.  $F$ -statistic and  $p$ -value are for the main effect in ANCOVA with control and learning nights as repeated measures and age as covariate. Delta, theta and gamma parameters are for all REMS epochs. M, mean; RMS, root-mean-square; SD, standard deviation. <sup>†</sup>Predicted by pre-sleep performance on learning task and age ( $F = 8.17$ ,  $R^2 = 0.70$ ,  $b = 0.22$ ,  $SE_b = 0.06$ ,  $\beta = 0.83$ ,  $p = 0.015$ ).

Table 6

Prediction of overnight change in performance on learning task by NREMS relative oscillatory parameters during learning night ( $N = 10$ )

Parameters	Fz					Cz				
	F	R <sup>2</sup>	B (SE)	$\beta$	P	F	R <sup>2</sup>	B (SE)	$\beta$	P
<b>Slow wave</b>										
Density	1.56	0.31	-0.026 (0.024)	-0.42	0.31	1.34	0.28	0.002 (0.002)	0.32	0.40
Duration	2.74	0.44	-0.091 (0.052)	-0.54	0.12	1.72	0.33	-0.62 (0.052)	-0.41	0.27
RMS	5.89	0.63	-0.32 (0.11)	-0.83	0.024*	3.26	0.48	-0.20 (0.10)	-0.60	0.089
Amplitude	2.54	0.42	-0.37 (0.22)	-0.61	0.14	2.14	0.38	-0.24 (0.16)	-0.45	0.19
Delta power, normalized	0.96	0.22	0.15 (0.33)	0.45	0.67	1.96	0.36	0.20 (0.15)	0.44	0.22
<b>Spindle</b>										
Density	0.92	0.21	-0.045 (0.12)	-0.12	0.73	1.01	0.22	0.041 (0.078)	0.18	0.62
Duration	1.13	0.24	-0.15 (0.22)	-0.25	0.51	0.95	0.21	0.093 (0.21)	0.15	0.68
RMS	0.86	0.20	0.013 (0.064)	0.07	0.85	1.13	0.24	-0.052 (0.076)	-0.24	0.51
Sigma power, normalized	1.15	0.25	0.032 (0.045)	0.32	0.50	1.44	0.29	-0.032 (0.032)	-0.38	0.36

Note. *F*-statistic,  $R^2$  and *p*-value are for the overall regression model with the oscillatory parameter and age as IVs. *B* (SE),  $\beta$  and *p*-value are for the oscillatory parameter. Learning night oscillatory parameters are normalized with respect to control night parameters (learning divided by control). DV is the change in performance, expressed as a ratio (0-1) of the total number of the word pairs presented.  $\beta$ , standardized coefficient, *B*, unstandardized coefficient,  $R^2$ , proportion of explained variance, RMS, root-mean-square; SE, standard error. \* $p < .05$ .

Table 7

Prediction of overnight change in performance on learning task by REMS relative oscillatory parameters during learning night ( $N = 10$ )

Parameters	Fz					Cz				
	F	R <sup>2</sup>	B (SE)	$\beta$	P	F	R <sup>2</sup>	B (SE)	$\beta$	P
<b>Delta train</b>										
Density	4.50	0.56	-0.022 (0.009)	-0.70	0.045*	5.18	0.60	-0.019 (0.007)	-0.71	0.033*
Duration	2.28	0.40	0.17 (0.11)	0.48	0.17	2.94	0.46	0.16 (0.09)	0.54	0.11
RMS	2.72	0.44	0.19 (0.01)	0.50	0.13	4.99	0.60	0.041 (0.016)	0.64	0.036*
Delta power, normalized	1.54	0.31	-0.033 (0.031)	-0.44	0.32	2.61	0.43	-0.047 (0.027)	-0.70	0.13
<b>Theta train</b>										
Density	2.25	0.39	-0.032 (0.021)	-0.48	0.17	4.60	0.57	-0.062 (0.025)	-0.63	0.043*
Duration	0.93	0.21	0.049 (0.12)	0.14	0.70	1.66	0.32	0.17 (0.15)	0.41	0.29
RMS	3.15	0.48	0.023 (0.01)	0.53	0.095	3.73	0.52	0.026 (0.01)	0.57	0.067
Theta power, normalized	1.75	0.33	-0.024 (0.015)	-0.47	0.26	2.29	0.17	-0.024 (0.016)	-0.52	0.17
Gamma power, normalized	3.02	0.46	-0.028 (0.015)	-0.52	0.10	1.06	0.23	-0.013 (0.021)	-0.20	0.57

Note.  $F$ -statistic,  $R^2$  and  $p$ -value are for the overall regression model with the oscillatory parameter and age as IVs.  $B$  (SE),  $\beta$  and  $p$ -value are for the oscillatory parameter. Learning night oscillatory parameters are normalized with respect to control night parameters (learning divided by control). DV is the change in performance, expressed as a ratio (0-1) of the total number of the word pairs presented.  $\beta$ , standardized coefficient,  $B$ , unstandardized coefficient,  $R^2$ , proportion of explained variance, RMS, root-mean-square; SE, standard error. \* $p < .05$ .

Table 8

*Average oscillatory event density per 30-s epoch, by participant*

<b>Participant</b>	<b>Slow wave</b>	<b>Spindle</b>	<b>Delta train</b>	<b>Theta train</b>
1	1.03 (0.41)	1.84 (0.11)	2.17 (1.40)	1.42 (0.49)
2	1.22 (0.08)	1.94 (0.13)	3.10 (0.67)	1.55 (0.11)
3	0.29 (0.08)	1.84 (0.22)	2.51 (0.24)	1.80 (0.18)
4	1.76 (0.15)	1.65 (0.11)	3.15 (0.22)	1.71 (0.10)
5	2.39 (1.71)	1.50 (0.20)	2.53 (0.58)	1.64 (0.18)
6	1.62 (0.36)	1.99 (0.09)	2.86 (0.23)	1.53 (0.14)
7	0.84 (0.30)	1.95 (0.17)	3.15 (0.35)	1.90 (0.14)
8	0.69 (0.23)	1.36 (0.29)	2.59 (0.27)	1.85 (0.23)
9	2.13 (0.59)	1.89 (0.07)	2.87 (0.51)	1.52 (0.15)
10	3.94 (0.75)	1.68 (0.10)	2.43 (0.21)	1.90 (0.10)
Mean (SD)	1.59 (1.05)	1.76 (0.21)	2.73 (0.34)	1.68 (0.18)

*Note.* Slow wave and spindle densities are for all N2 and N3 epochs. Delta and theta train densities are for all REMS epochs. Means are presented, with SDs in parentheses.

Table 9

Comparison of MI on experimental nights ( $N = 10$ )

Band pair	Fz				Cz			
	Control M (SD)	Learning M (SD)	F	P	Control M (SD)	Learning M (SD)	F	P
<b>NREMS</b>								
$\delta - \sigma$	-5.69 (0.20)	-5.68 (0.20)	0.21	0.66	-5.59 (0.20)	-5.58 (0.20)	0.35	0.57
$\delta - \sigma$ , NP1	-5.80 (0.23)	-5.86 (0.26)	0.17	0.69	-5.70 (0.26)	-5.63 (0.22)	4.94	0.057
<b>REMS</b>								
$\delta - \gamma$	-7.04 (0.41)	-7.07 (0.32)	0.94	0.36	-7.08 (0.40)	-7.13 (0.30)	1.99	0.20
$\theta - \gamma$	-7.71 (0.34)	-7.73 (0.35)	1.93	0.20	-7.80 (0.31)	-7.80 (0.30)	0.92	0.37

Note.  $F$ -statistic and  $p$ -value are for main effect in ANCOVA with control and learning nights as repeated measures and age as covariate. MIs were log-transformed.  $\gamma$ , gamma (50-100 Hz);  $\delta$ , delta (0.25-4 Hz in NREMS; 1.5-3.5 Hz in REMS);  $\theta$ , theta (3.5-8 Hz);  $\sigma$ , adapted sigma; M, mean; MI, modulation index; NP1, NREMS period 1.

Table 10

Prediction of overnight change in performance on learning task by relative MI during learning night ( $N = 10$ )

Band pair	Fz					Cz				
	F	R <sup>2</sup>	B (SE)	$\beta$	P	F	R <sup>2</sup>	B (SE)	$\beta$	P
<b>NREMS</b>										
$\delta - \sigma$	1.81	0.34	0.34 (0.27)	0.39	0.25	0.85	0.20	0.37 (0.25)	0.051	0.89
$\delta - \sigma$ , NP1	11.42	0.77	0.51 (0.12)	0.77	0.004**	1.02	0.23	-0.13 (0.24)	-0.23	0.60
<b>REMS</b>										
$\delta - \gamma$	2.71	0.44	-0.32 (0.18)	-0.53	0.13	4.68	0.57	-0.35 (0.14)	-0.70	0.041*
$\theta - \gamma$	8.91	0.72	-0.47 (0.13)	-0.82	0.009**	2.23	0.39	-0.24 (0.16)	-0.47	0.18

Note.  $F$ -statistic,  $R^2$  and  $p$ -value are for the overall regression model with MI and age as IVs.  $B$  (SE),  $\beta$  and  $p$ -value are for the MI. Learning night MI was log-transformed, then normalized with respect to control night log MI (learning divided by control). DV is the change in performance, expressed as a ratio (0-1) of the absolute pre-to-post change in the number of word pairs recalled over the total number of the word pairs presented.  $\beta$ , standardized coefficient  $\gamma$ , gamma (50-100 Hz);  $\delta$ , delta (0.25-4 Hz in NREMS; 1.5-3.5 Hz in REMS);  $\theta$ , theta (3.5-8 Hz);  $\sigma$ , adapted sigma; B, unstandardized coefficient; MI, modulation index; NP1, NREMS period 1;  $R^2$ , proportion of explained variance; SE, standard error. \* $p < .05$ . \*\* $p < .01$ .

Table 11

Prediction of MI during learning night by pre-sleep performance on learning task (N = 10)

Band pair	Fz					Cz				
	F	R <sup>2</sup>	B (SE)	β	P	F	R <sup>2</sup>	B (SE)	β	P
<b>NREMS</b>										
δ - σ	0.12	0.03	0.011 (0.04)	0.11	0.78	0.15	0.04	0.012 (0.05)	0.10	0.80
δ - σ, NP1	1.27	0.27	0.06 (0.04)	0.49	0.18	2.08	0.37	-0.16 (0.05)	-0.13	0.74
<b>REMS</b>										
δ - γ	0.54	0.13	0.02 (0.06)	0.10	0.78	1.07	0.23	-0.009 (0.06)	-0.05	0.88
θ - γ	1.10	0.24	-0.02 (0.05)	-0.16	0.64	0.58	0.14	0.021 (0.05)	-0.15	0.68

*Note.* *F*-statistic, *R*<sup>2</sup> and *p*-value are for the overall regression model with pre-sleep score and age as IVs. *B* (*SE*), *β* and *p*-value are for the pre-sleep score. Pre-sleep score was expressed as a ratio (0-1) of the number of words recalled to the total number of the word pairs presented. DV is the log-transformed learning night MI. *β*, standardized coefficient; *γ*, gamma (50-100 Hz); *δ*, delta (0.25-4 Hz in NREMS; 1.5-3.5 Hz in REMS); *θ*, theta (3.5-8 Hz); *σ*, adapted sigma; *B*, unstandardized coefficient; MI, modulation index; NP1, NREMS period 1; *R*<sup>2</sup>, proportion of explained variance; SE, standard error.

Table 12

Comparison of power-triggered MI on experimental nights (N=10)

Band pair	Fz				Cz			
	Control	Learning	F	P	Control	Learning	F	P
	M (SD)	M (SD)			M (SD)	M (SD)		
<b>NREMS</b>								
$\delta - \sigma$ , NP1	-6.06 (0.75)	-6.16 (1.36)	6.51	0.034*	-5.42 (0.63)	-5.52 (1.07)	3.39	0.10
<b>REMS</b>								
$\delta - \gamma$	-6.28 (1.08)	-6.17 (0.79)	0.60	0.46	-6.49 (1.08)	-6.30 (1.26)	0.024	0.88
$\theta - \gamma$	-6.91 (1.02)	-6.70 (1.03)	0.81	0.39	-6.96 (0.72)	-6.79 (0.93)	0.64	0.45

*Note.* F-statistic and p-value are for main effect in ANCOVA with control and learning nights as repeated measures and age as covariate. MIs were log-transformed.  $\gamma$ , gamma (50-100 Hz);  $\delta$ , delta (0.25-4 Hz in NREMS; 1.5-3.5 Hz in REMS);  $\theta$ , theta (3.5-8 Hz);  $\sigma$ , adapted sigma; M, mean; MI, modulation index; NP1, NREMS period 1. \* $p < .05$ .

Table 13

Prediction of overnight change in performance on learning task by relative power-triggered MI  
( $N = 10$ )

Band pair	Fz					Cz				
	F	R <sup>2</sup>	B (SE)	$\beta$	P	F	R <sup>2</sup>	B (SE)	$\beta$	P
<b>NREMS</b>										
$\delta - \sigma$ , NP1	1.21	0.26	0.036 (0.046)	0.34	0.46	0.88	0.20	-0.013 (0.051)	-0.10	0.80
<b>REMS</b>										
$\delta - \gamma$	2.85	0.45	-0.082 (0.045)	-0.54	0.11	2.06	0.37	-0.003 (0.002)	-0.45	0.18
$\theta - \gamma$	1.16	0.25	-0.041 (0.056)	-0.25	0.50	0.88	0.20	0.017 (0.060)	0.01	0.79

*Note.*  $F$ -statistic,  $R^2$  and  $p$ -value are for the overall regression model with MI and age as IVs.  $B$  (SE),  $\beta$  and  $p$ -value are for the MI. Learning night MI was log-transformed, then normalized with respect to control night log MI (learning divided by control). DV is the change in performance, expressed as a ratio (0-1) of the absolute pre-to-post change in the number of word pairs recalled over the total number of the word pairs presented.  $\beta$ , standardized coefficient;  $\gamma$ , gamma (50-100 Hz);  $\delta$ , delta (0.25-4 Hz in NREMS; 1.5-3.5 Hz in REMS);  $\theta$ , theta (3.5-8 Hz);  $\sigma$ , adapted sigma; B, unstandardized coefficient; MI, modulation index; NP1, NREMS period 1;  $R^2$ , proportion of explained variance; SE, standard error.

Table 14

*Prediction of overnight change in performance on learning task by relative phase-binned MA (N = 10)*

Parameter	Fz					Cz				
	F	R <sup>2</sup>	B (SE)	β	P	F	R <sup>2</sup>	B (SE)	β	P
MA over trough	2.28	0.40	-0.17 (0.11)	-0.53	0.17	5.35	0.61	-0.21 (0.78)	-0.71	0.031*
MA over peak	1.86	0.60	-0.16 (0.12)	-0.40	0.24	2.08	0.37	-0.16 (0.11)	-0.43	0.20

*Note.* *F*-statistic, *R*<sup>2</sup> and *p*-value are for the overall regression model with MA and age as IVs. *B* (SE), *β* and *p*-value are for the MA. Learning night MA was log-transformed, then normalized with respect to control night log MA (learning divided by control). DV is the change in performance, expressed as a ratio (0-1) of the absolute pre-to-post change in the number of word pairs recalled over the total number of the word pairs presented. MAs are for NREMS period 1 only. *β*, standardized coefficient, *B*, unstandardized coefficient, MA, mean amplitude, *R*<sup>2</sup>, proportion of explained variance, SE, standard error. \**p* < .05.

Table 15

Comparison of comodulogram MI on experimental nights on Cz (N=10)

Phase band (Hz)	Amplitude band (Hz)	Control M (SD)	Learning M (SD)	T	P
<b>REMS</b>					
$\delta - \gamma$					
1.5 – 1.8	67.7 – 70.3	0.816 (0.088)	0.908 (0.086)	2.69	0.025*
1.8 – 2.0	57.4 – 61.4	1.077 (0.118)	0.978 (0.070)	-2.59	0.029*
$\theta - \beta/\gamma$					
4.3 – 5.0	22.1 – 33.1	0.984 (0.055)	1.058 (0.078)	2.29	0.048*
4.3 – 5.0	27.6 – 37.6	0.947 (0.037)	1.065 (0.086)	4.70	0.0011**
5.0 – 5.8	22.1 – 33.1	0.972 (0.026)	1.059 (0.094)	2.83	0.020*
5.0 – 5.8	27.6 – 37.6	0.983 (0.048)	1.031 (0.071)	1.92	0.087
6.8 – 7.8	30.0 – 45.7	0.971 (0.042)	1.051 (0.077)	3.04	0.014*
$\beta - \gamma$					
10.6 – 12.3	38.8 – 63.4	1.086 (0.090)	1.015 (0.059)	-2.54	0.032*
14.3 – 16.6	27.4 – 60.6	1.011 (0.063)	1.080 (0.081)	3.26	0.0098**
<b>NREMS</b>					
$\delta - \beta/\gamma$					
1.8 – 2.0	57.4 – 61.4	0.933 (0.065)	1.017 (0.11)	2.88	0.018*
2.0 – 2.4	18.4 – 23.2	1.043 (0.091)	0.951 (0.075)	-2.53	0.032*
2.0 – 2.4	21.8 – 26.6	0.999 (0.073)	0.919 (0.082)	-2.55	0.031*
2.0 – 2.4	41.6 – 46.4	0.994 (0.058)	0.935 (0.034)	-2.60	0.029*
2.7 – 3.2	29.4 – 35.8	0.980 (0.067)	0.906 (0.062)	-2.33	0.045*
$\theta - \gamma$					
3.7 – 4.3	64.7 – 73.3	1.016 (0.074)	0.960 (0.040)	-2.38	0.041*
5.0 – 5.8	63.2 – 74.8	1.033 (0.081)	0.936 (0.063)	-2.59	0.029*
6.8 – 7.8	51.6 – 67.2	1.056 (0.062)	0.996 (0.033)	-2.71	0.024*
6.8 – 7.8	72.4 – 88.0	1.043 (0.061)	0.952 (0.059)	-3.14	0.012*

Note. *t*-statistics and *p*-values are for paired samples *t*-tests. MIs were log-transformed, and divided by the average of all MIs for that participant, experimental night and stage.  $\beta$ , beta;  $\gamma$ , gamma;  $\delta$ , delta;  $\theta$ , theta; M, mean; MI, modulation index. \**p* < .05. \*\**p* < .01

## Figures

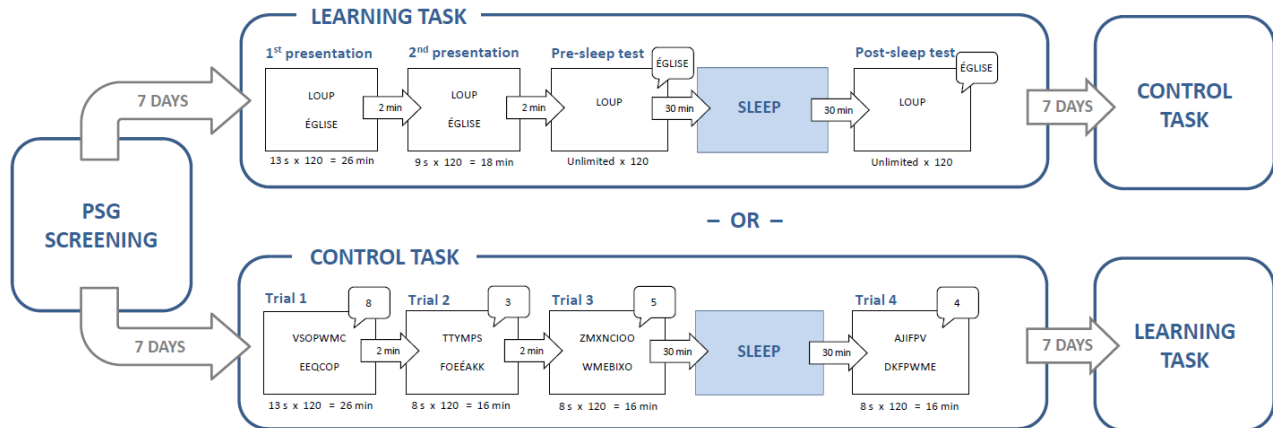


*Figure 1.* Schematic of the study design. Participants underwent a first night of PSG screening, followed 7 days later by either a learning night or a control night, counterbalanced between participants. Both experimental nights consisted of three pre-sleep phases and one post-sleep phase. In the learning task, participants were presented with 120 word pairs twice each, then had to recall the learned association during pre-sleep and post-sleep test phases. In the control task, participants had to simply count the number of curved letters (e.g. J, P, C) on-screen and report the total. Participants completed the other task on a 3<sup>rd</sup> night, 7 days later.

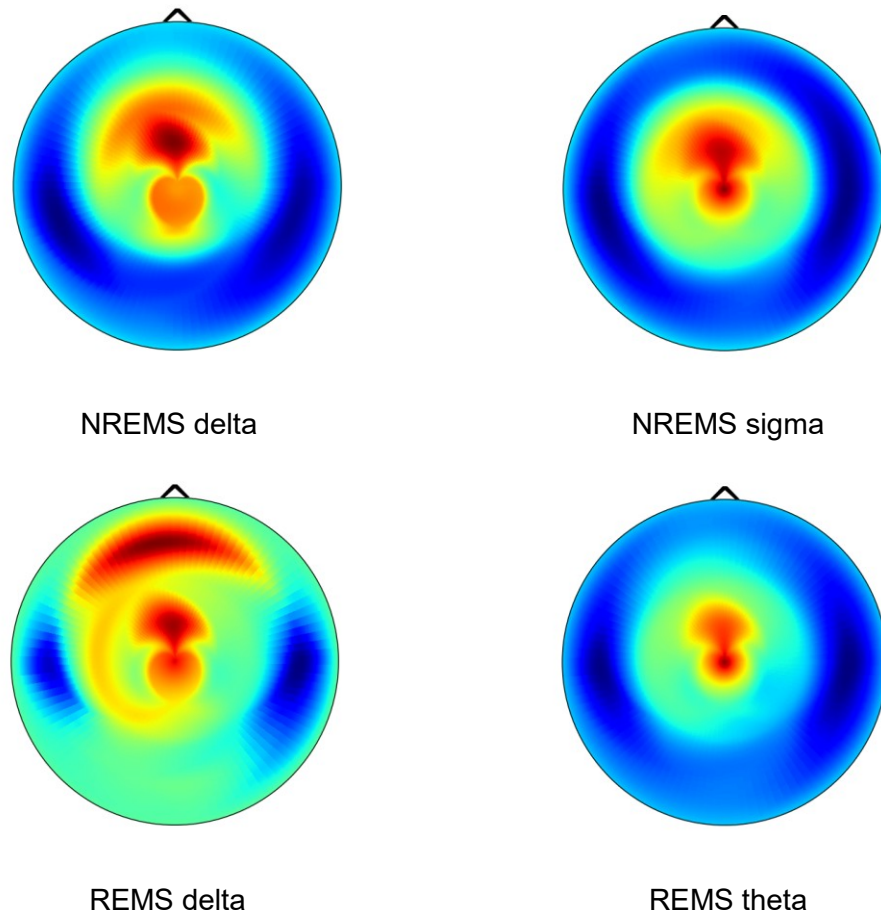


*Figure 2.* Topographical head maps of raw power spectral density means for NREMS delta (0.5-4 Hz) and sigma (10-16 Hz), and REMS delta (1.5-3.5 Hz) and theta (4-8 Hz), across 16 electrodes and 9 participants (both nights averaged). The nasion is indicated by the upper triangle. Cz and Fz show the greatest spectral power in all cases.

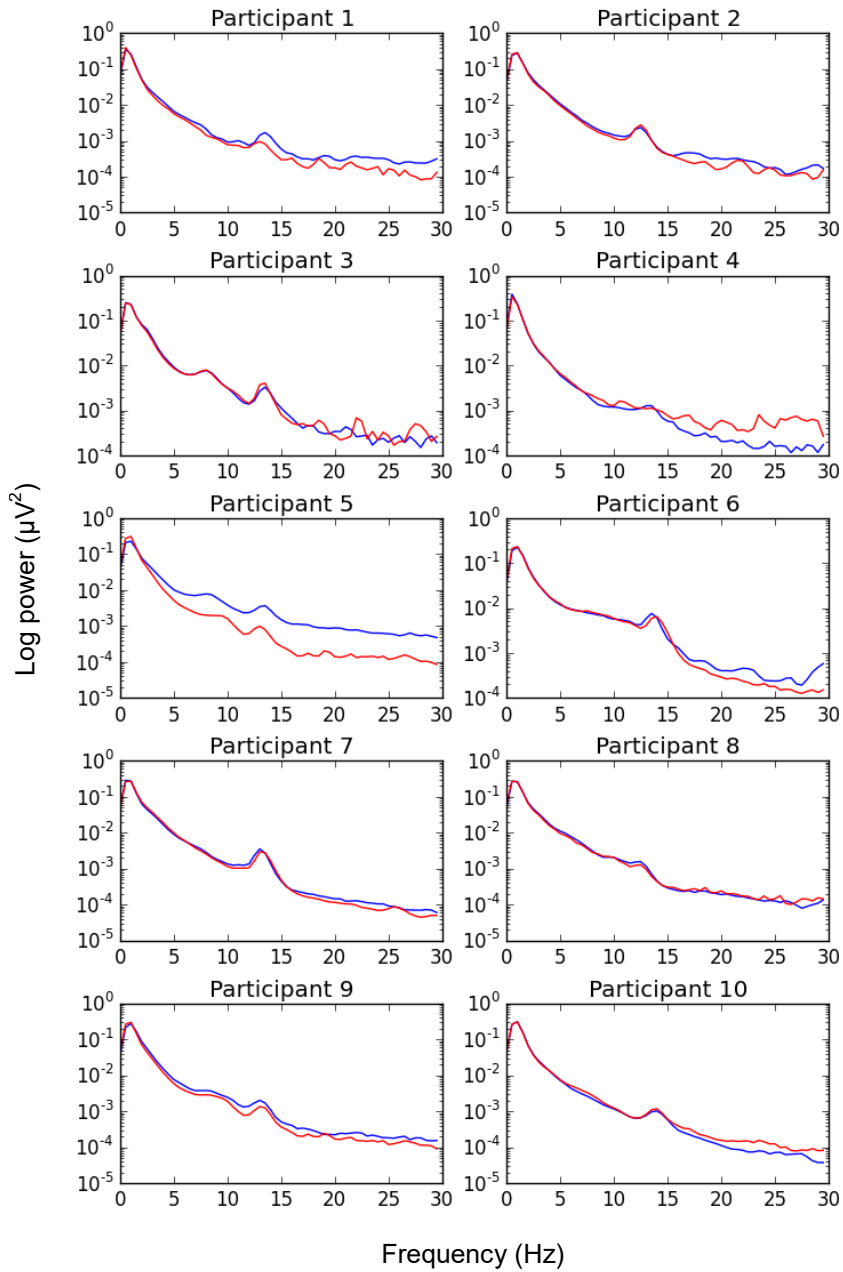


Figure 3. NREMS power spectral densities for all participants, in NP1 only. Learning nights are in red and control nights in blue. Note the clear peaks in delta and sigma power. NP1, NREMS period 1.

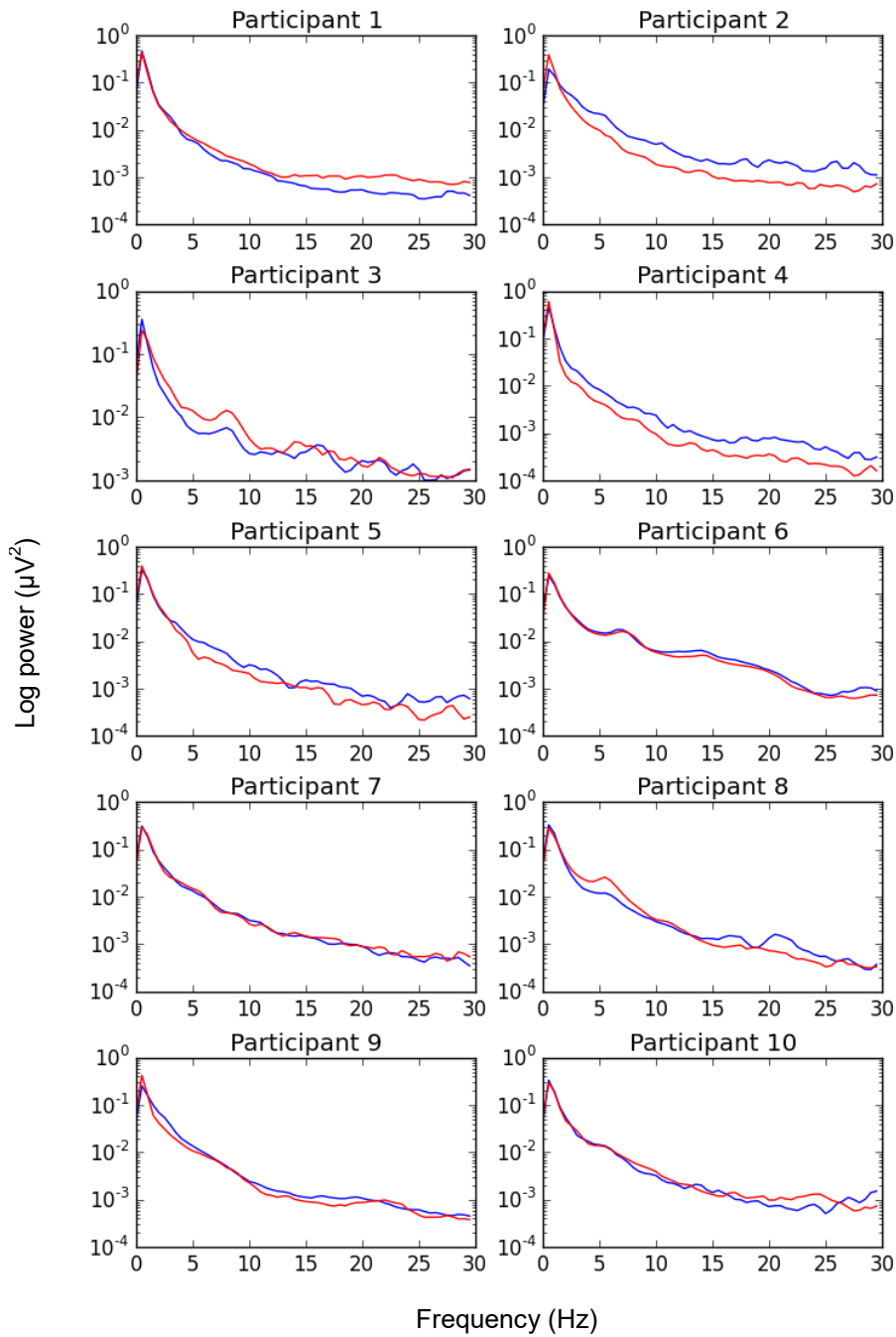
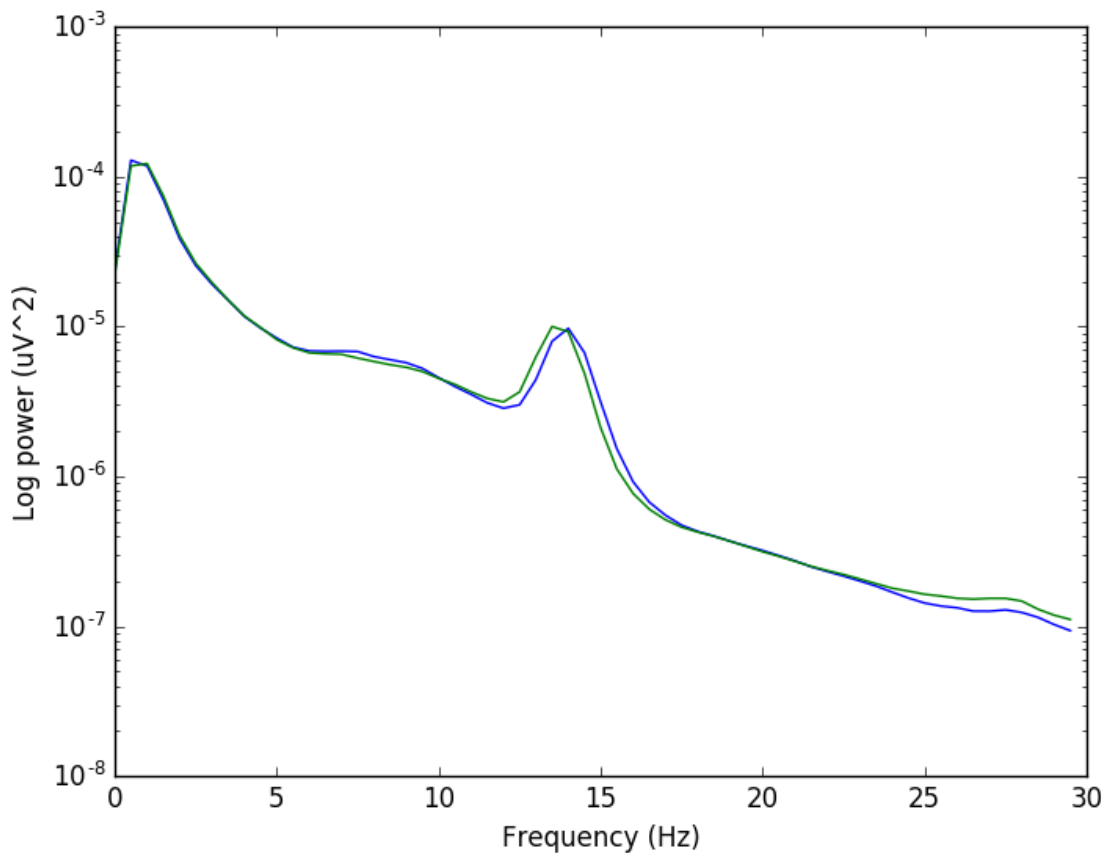


Figure 4. REMS power spectral densities for all participants. Learning nights are in red and control nights in blue. Note the clear peaks in theta power in participants 3, 6, 8 and 10.



*Figure 5.* Power spectral density of all stage N2 epochs, concatenated, for one participant on experimental nights. Blue is the learning night, and green is the control night. Note the close agreement in peaks in the sigma range. The average of these two peaks for each participant was taken as the adapted sigma centre frequency.

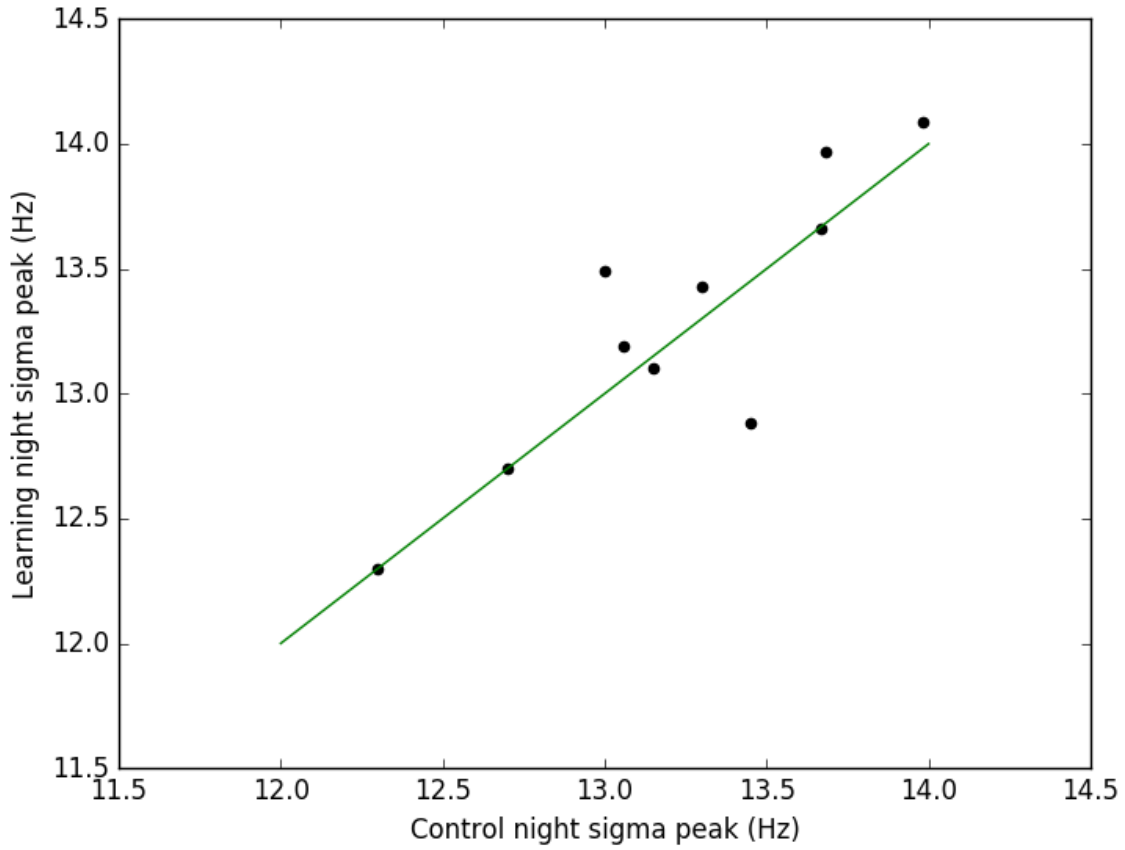
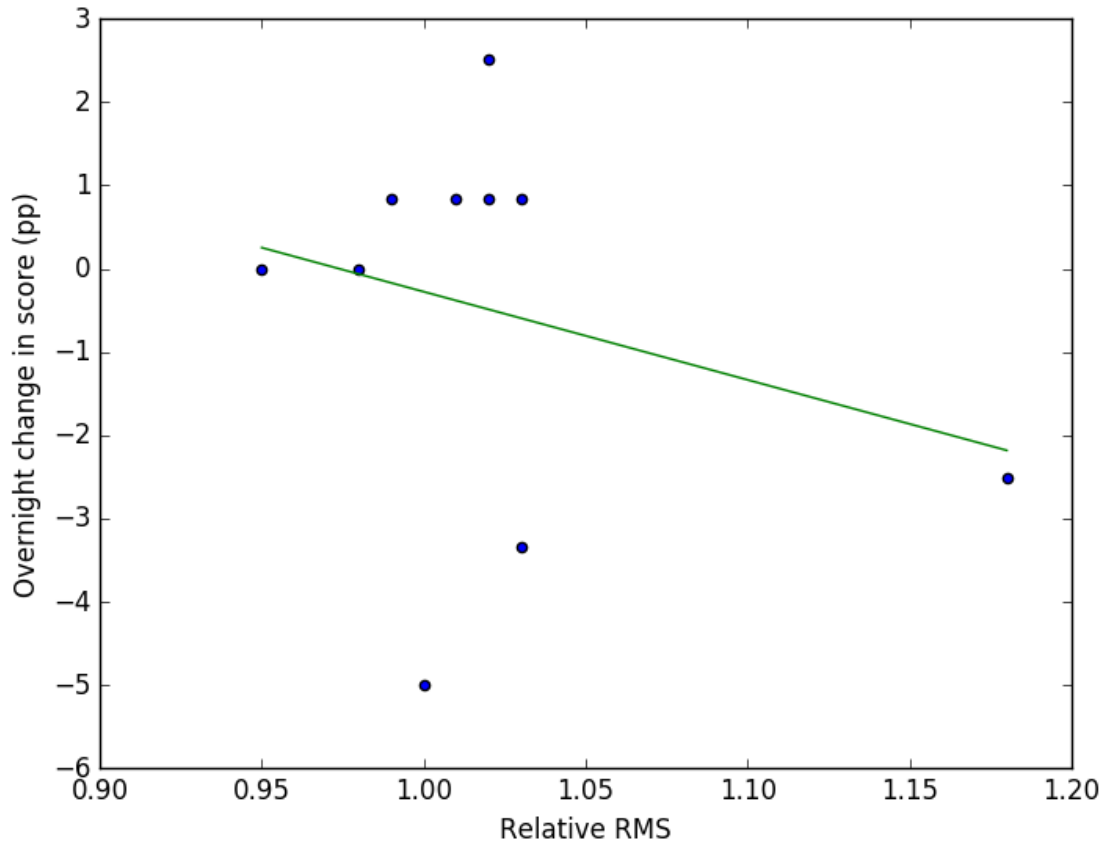
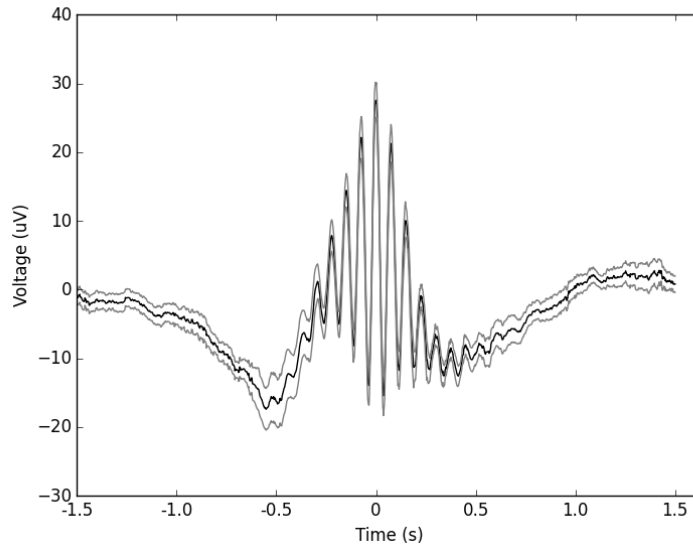


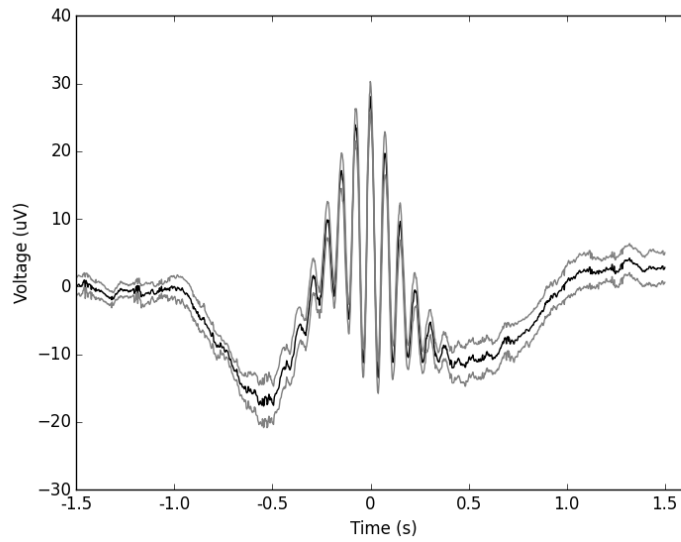
Figure 6. Correlation between stage N2 sigma peaks per participant on experimental nights (N = 10). The green line indicates equality.



*Figure 7.* Correlation between slow wave relative RMS during stages N2 and N3 on Fz and overnight change in word pair recall (N = 10). Relative RMS is the learning night RMS divided by the control night value. The correlation is driven by an outlier. RMS, root-mean-square.



Control



Learning

*Figure 8.* Grand average of all detected spindles for all participants during NREMS (all periods) in control and learning nights, centered at the most negative trough ( $\pm$  SEM). The spindle is visibly coupled to the rising phase of the SW. SEM, standard error of the mean; SW, slow wave.

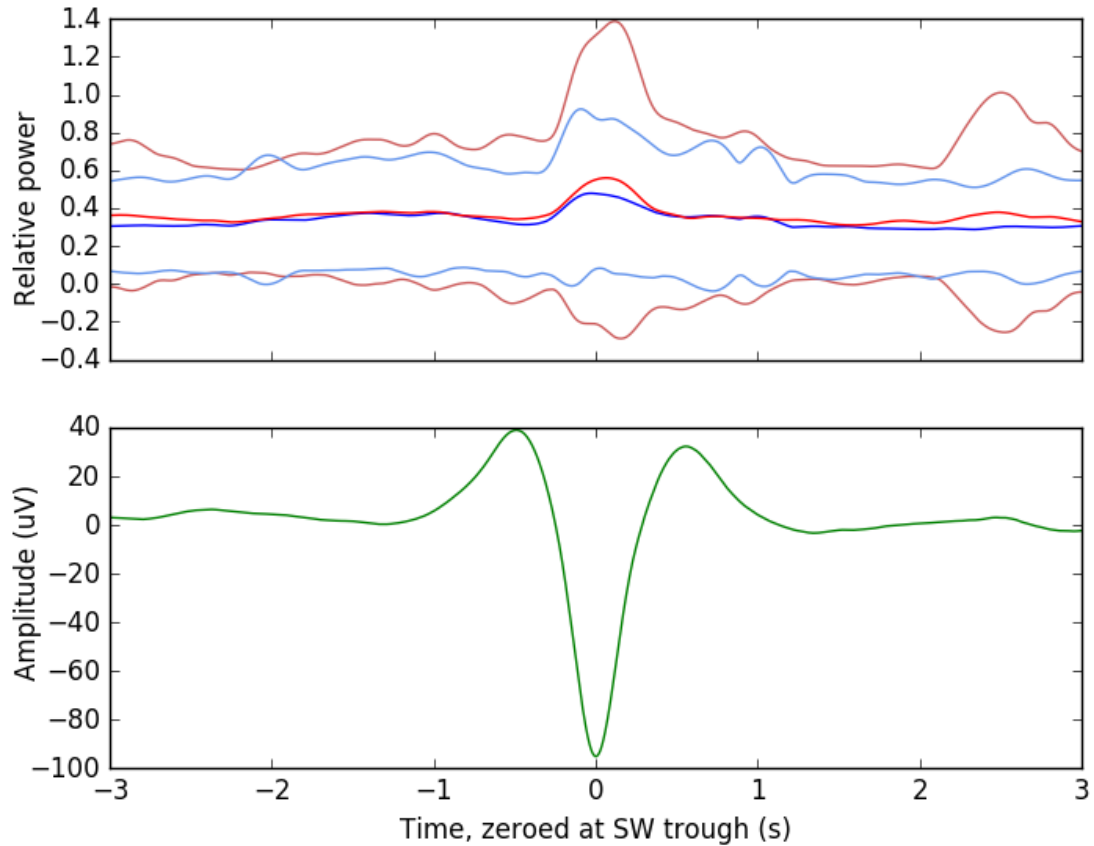
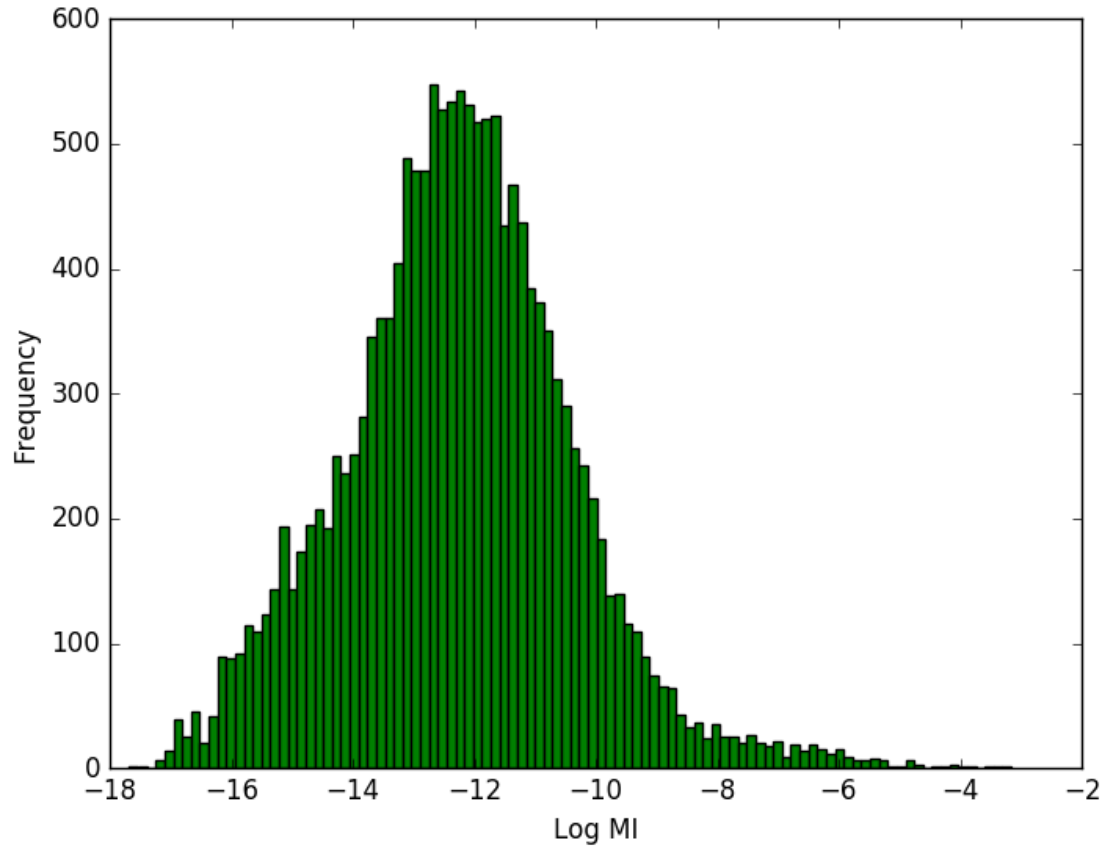
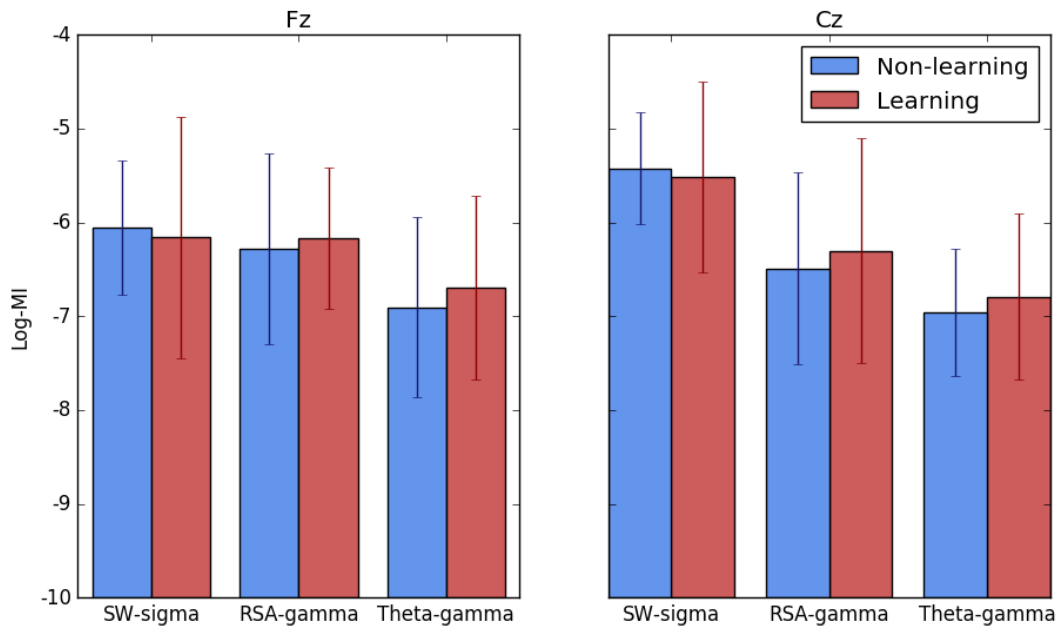


Figure 9. SW trough-triggered adapted sigma average amplitude envelope on experimental nights, over average SW, on Cz (N = 10). Red is learning night sigma power, blue is control night sigma power, and green is the average SW signal. Dark lines are the mean, and light lines are the  $\pm$  standard deviation. Raw signal during all automatically detected SWs was filtered within the adapted sigma band, Hilbert-transformed to obtain the amplitude envelope, averaged for each participant, and normalized with respect to that participant's pre-sleep, pre-task quiet wakefulness recording RMS. Average amplitude envelopes were then averaged for each experimental night, across participants. SW, slow wave.



*Figure 10.* Histogram of natural logarithm-transformed MIs (N = 16200). The frequency distribution approximates the Gaussian. MIs were taken from the comodulogram analysis. The heavy tail on the right is likely due to artefacts from the comodulogram. MI, modulation index.



*Figure 11.* Comparison of log-transformed modulation index between experimental nights, by band pair and electrode (N = 10). SW-sigma is for NREMS period 1. RSA (delta)-gamma and theta-gamma are for all REMS. Error bars indicate the standard deviation. RSA, rhythmic slow activity; SW, slow wave.

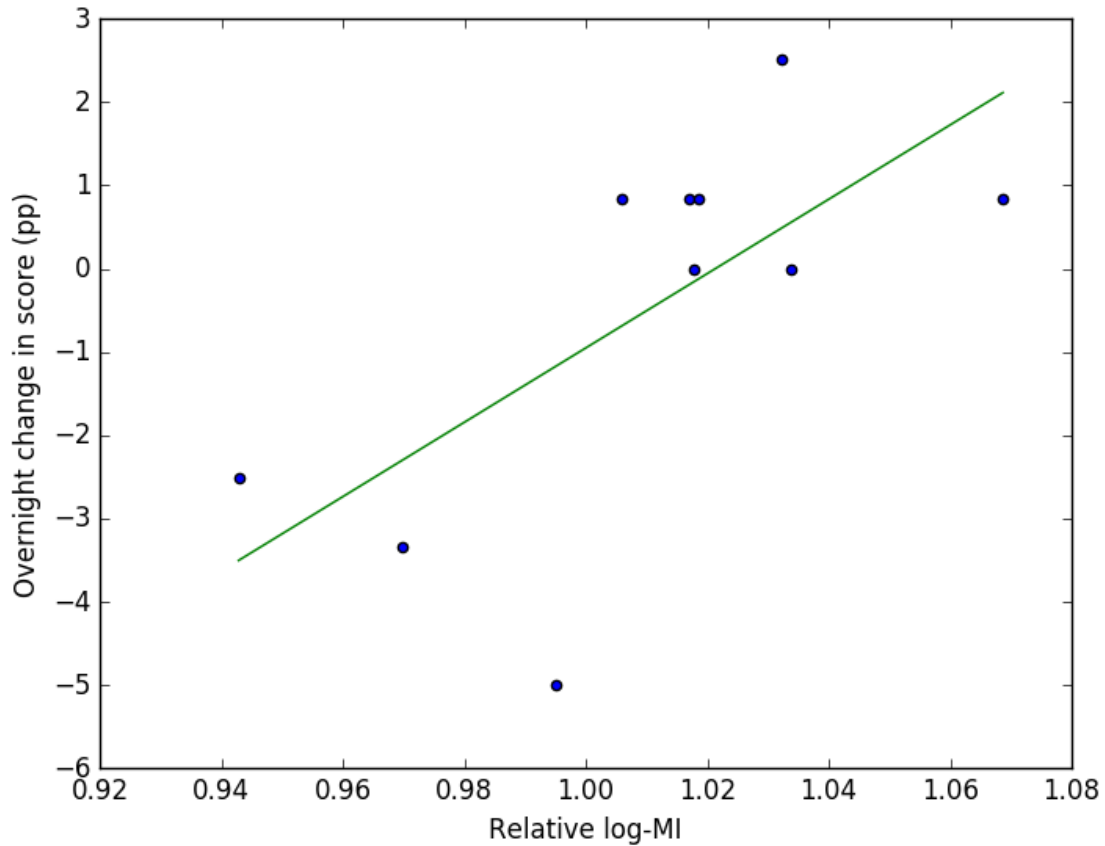
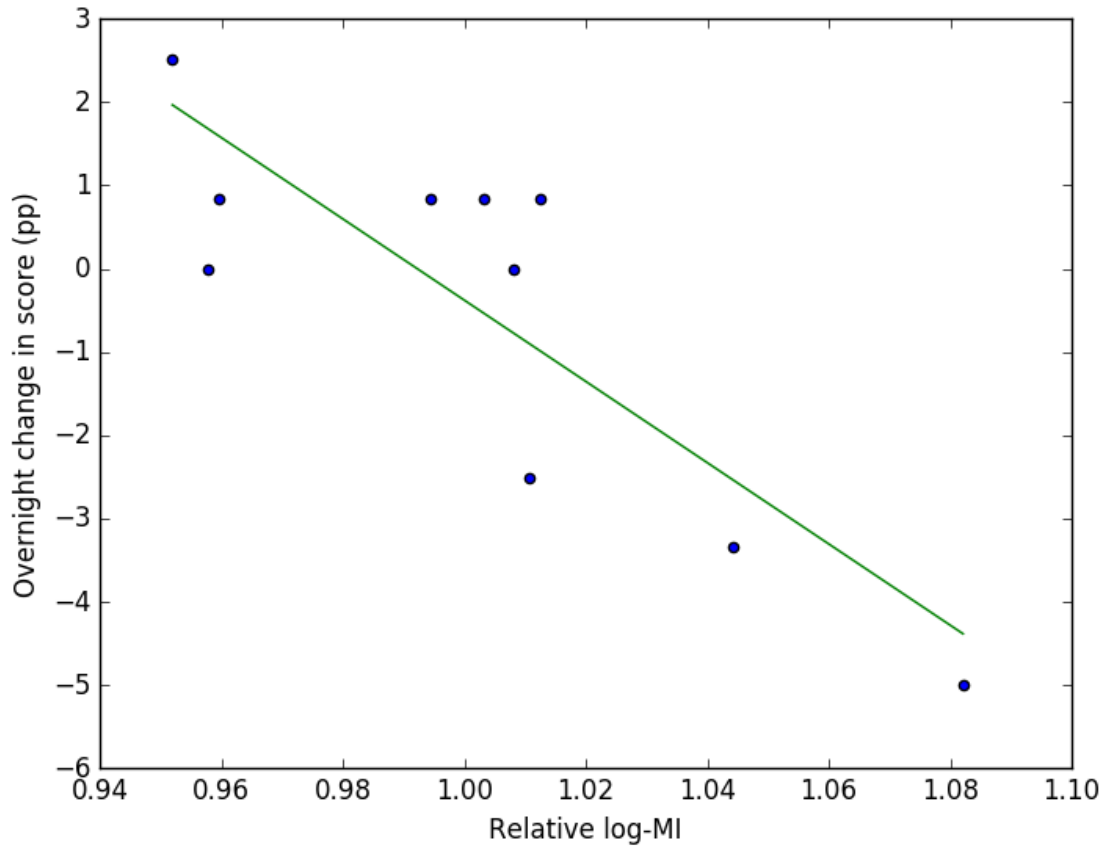
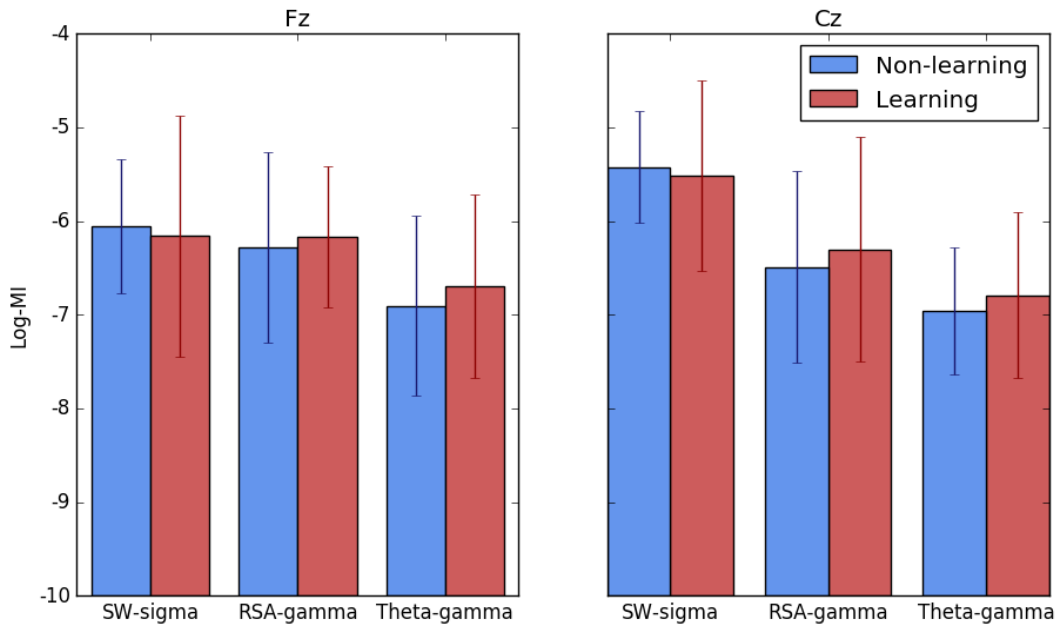


Figure 12. Correlation between relative log-transformed delta-sigma MI in NREMS period 1 on Fz and overnight change in word pair recall (N = 10). Delta (0.25-4 Hz) was the phase-giving frequency, and adapted sigma the amplitude-giving frequency. Relative MI is the learning night MI divided by the control night value. Model 2 multiple regression revealed a significant prediction ( $F = 11.42$ ,  $R^2 = 0.77$ ,  $b = 51$ ,  $SE_b = 12$ ,  $\beta = 0.77$ ,  $p_{MI} = 0.004$ ). MI, modulation index.



*Figure 13.* Correlation between relative log-transformed theta-gamma MI in REMS on Fz and overnight change in word pair recall (N = 10). Theta (3.5-8 Hz) was the phase-giving frequency, and gamma (50-100 Hz) the amplitude-giving frequency. Relative MI is the learning night MI divided by the control night value. Model 2 multiple regression revealed a significant prediction ( $F = 8.91$ ,  $R^2 = 0.72$ ,  $b = -47$ ,  $SE_b = 13$ ,  $\beta = -0.82$ ,  $p_{MI} = 0.009$ ). MI, modulation index.



*Figure 14.* Comparison of log-transformed power-triggered modulation index between experimental nights, by band pair and electrode (N = 10). SW-sigma MI is for NREMS period 1 only. Delta-gamma MI and theta-gamma MI are for all REMS. Error bars indicate the standard deviation. RSA, rhythmic slow activity (delta); SW, slow wave.

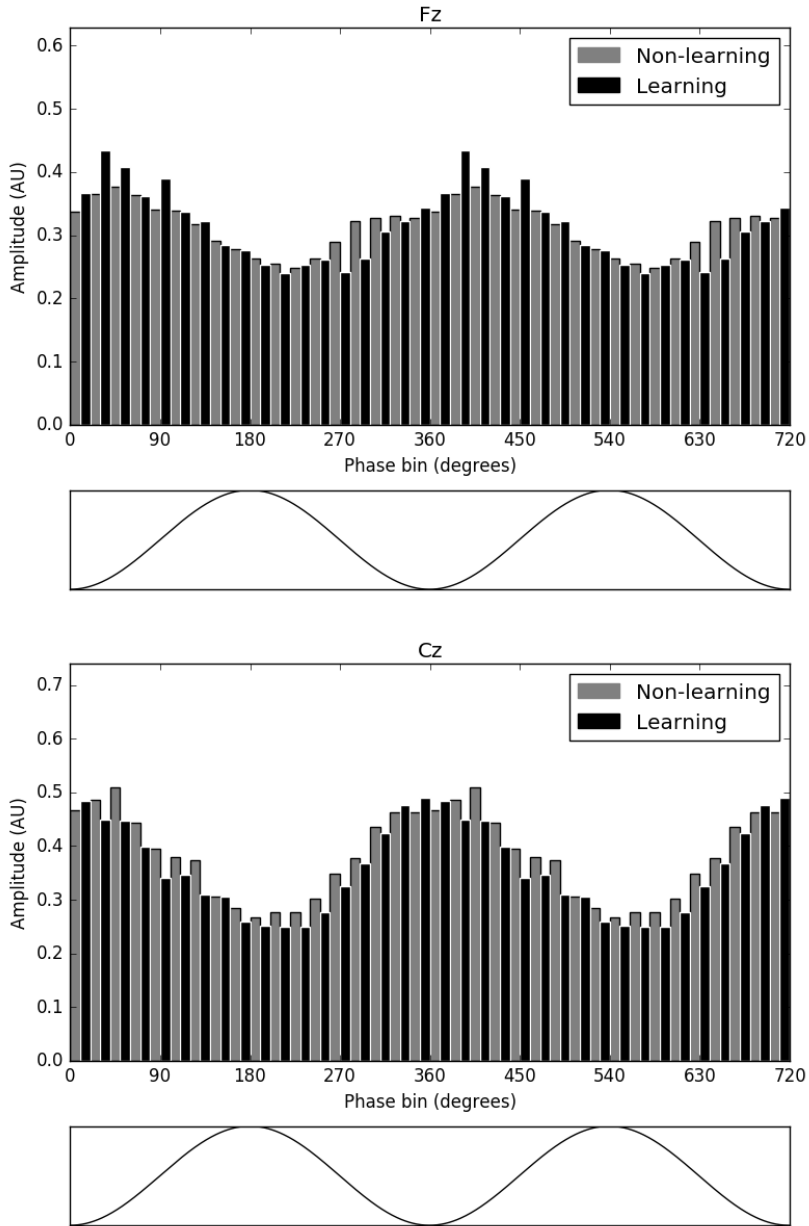


*Figure 15.* Phase-amplitude plots for participant 10 in NREMS period 1 comparing experimental nights. Mean amplitudes per phase bin (where  $0^\circ$  is the delta trough, corresponding to the SO down-state) were log-transformed and normalized with respect to the log-transformed mean amplitude of the pre-sleep, pre-task quiet wakefulness recording. The sinusoid below each plot illustrates the phase of the delta oscillation corresponding to each bin. AU, arbitrary unit; SW, slow wave.

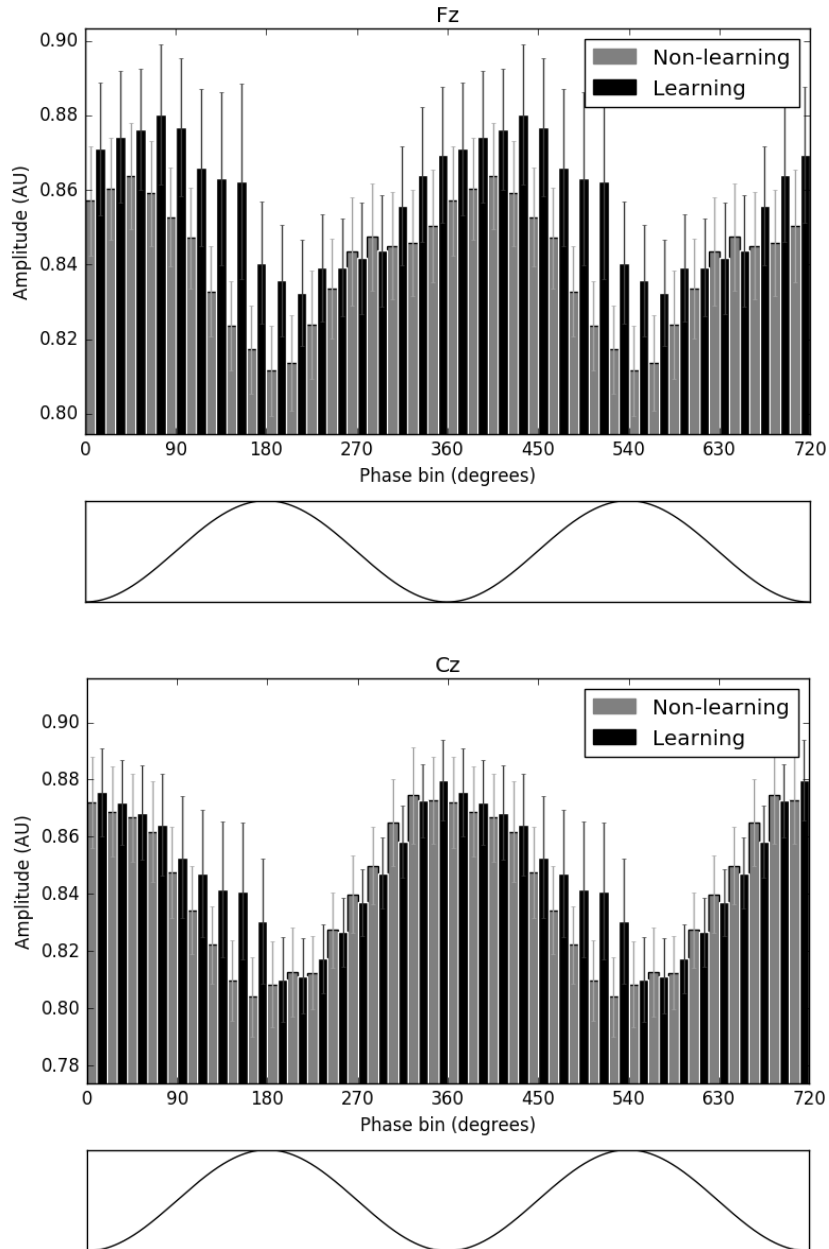


*Figure 16.* Average delta-sigma phase-amplitude plot in NREMS period 1 on experimental nights (N = 10). Mean amplitudes per phase bin (where 0° is the delta trough, corresponding to the SW up-state) were log-transformed and normalized with respect to the log-transformed mean amplitude of the pre-sleep, pre-task quiet wakefulness recording, then averaged across participants. Error bars represent the standard error of the mean. The sinusoid below each plot illustrates the phase of the delta oscillation corresponding to each bin. On learning nights, the phase-amplitude relationship seems smeared to the right. AU, arbitrary unit; SW, slow wave.

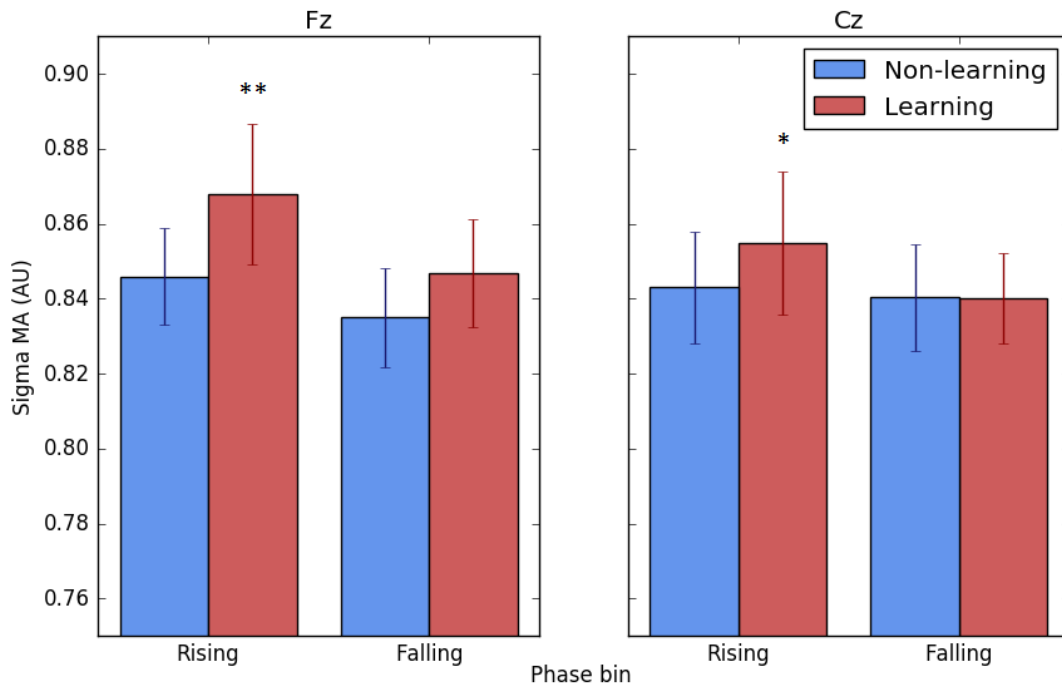
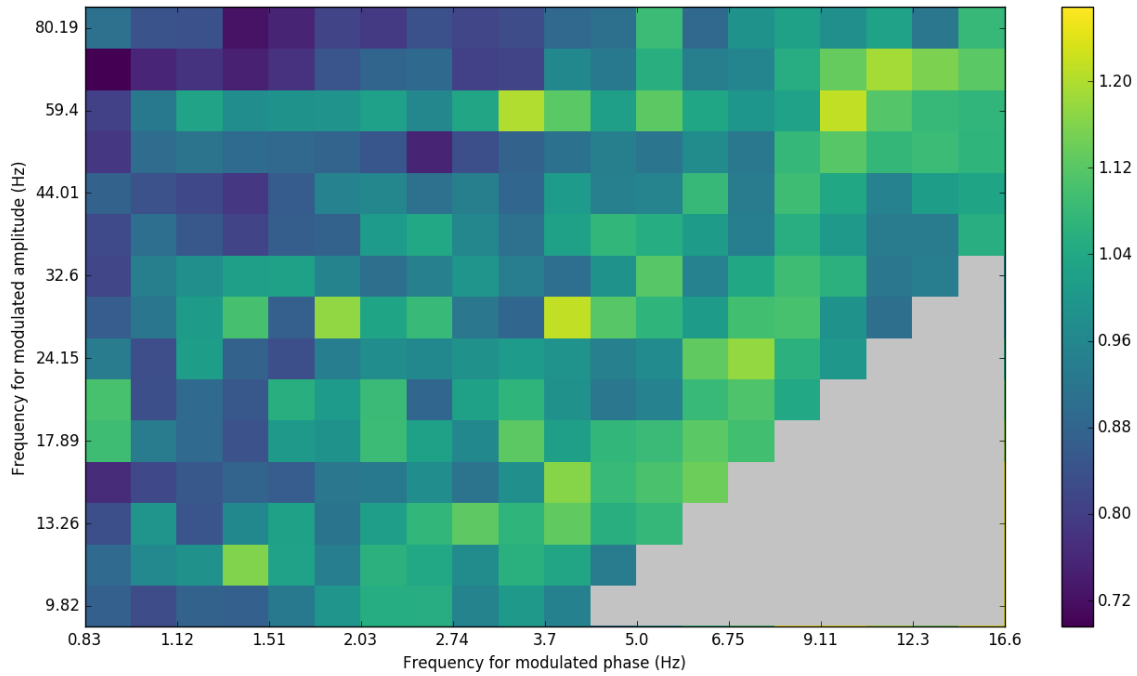
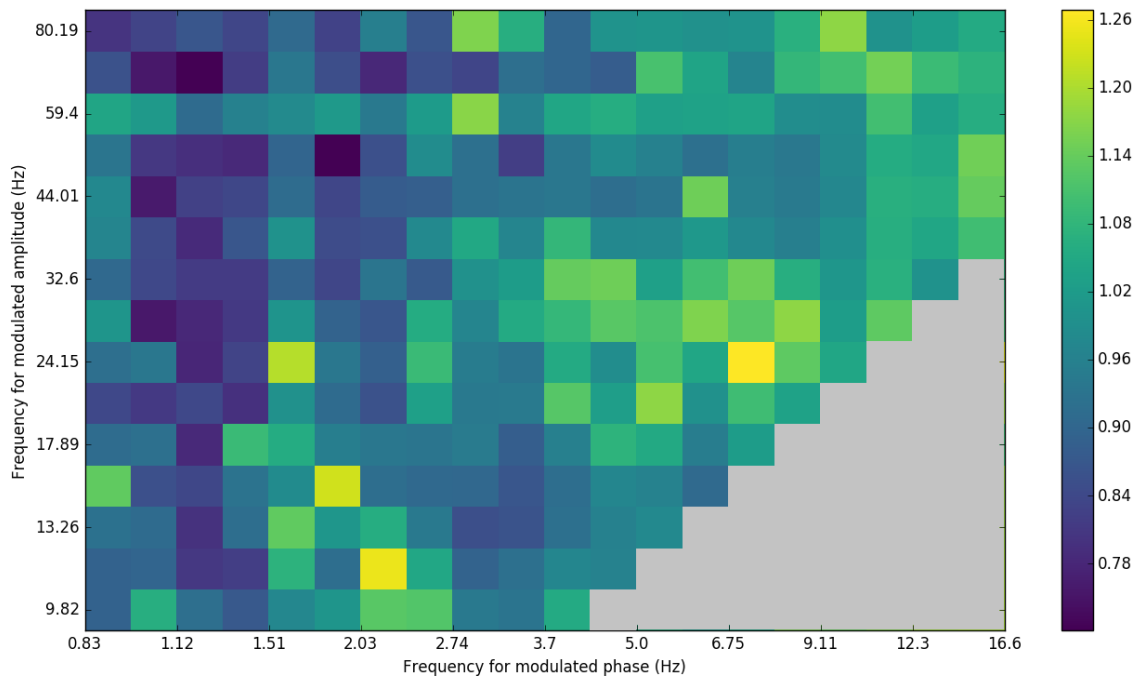


*Figure 17.* Comparison of mean amplitudes over rising and falling phases of delta during experimental nights (N = 10). Mean amplitudes per phase bin (rising or falling phase of SW) were log-transformed and normalized with respect to the log-transformed mean amplitude of the pre-sleep, pre-task quiet wakefulness recording, then averaged across participants. Error bars represent the standard error of the mean. Rising phase corresponds to the SW down-state transition, and falling phase to the up-state transition. AU, arbitrary unit; MA, mean amplitude; SW, slow wave. \* $p < 0.05$ , \*\* $p < 0.01$



NREMS



REMS

Figure 18. NREMS and REMS comodulograms for participant 1. Colours represent log-transformed MIs, normalized with respect to the comodulogram average. Bandwidths for the amplitude frequency are always double the upper limit of the phase frequency. MI, modulation index.

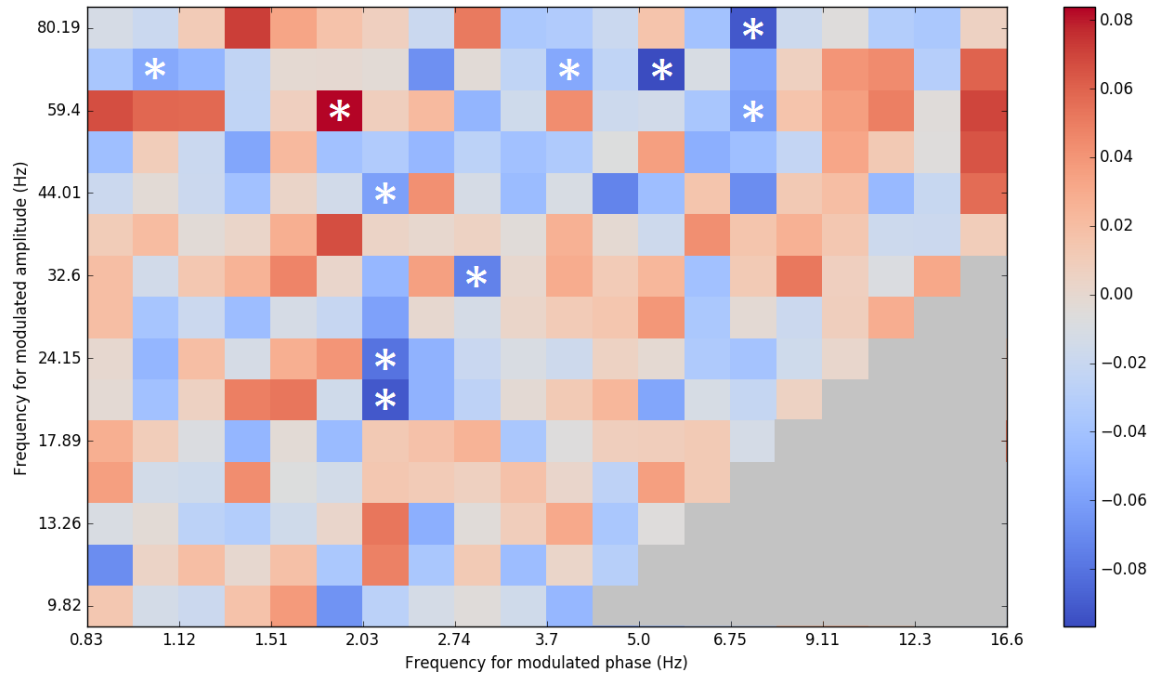


*Figure 19.* Difference comodulogram for NREMS period 1 (N = 10). Colours represent differences (learning minus non-learning) in normalized log-transformed MIs. Bandwidths for the amplitude frequency are always double the upper limit of the phase frequency. MI, modulation index. \* $p < 0.05$ .

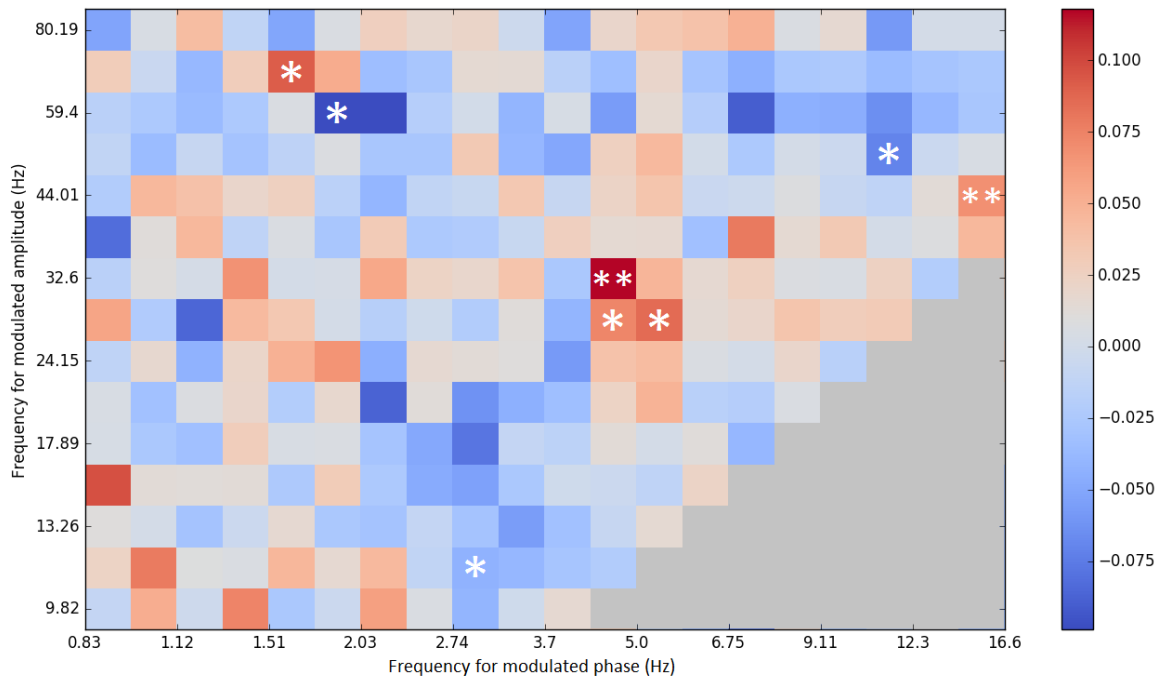


*Figure 20.* Difference comodulogram for REMS (N = 10). Colours represent differences (learning minus non-learning) in normalized log-transformed MIs. Bandwidths for the amplitude frequency are always double the upper limit of the phase frequency. MI, modulation index. \* $p < 0.05$ , \*\* $p < 0.01$ .

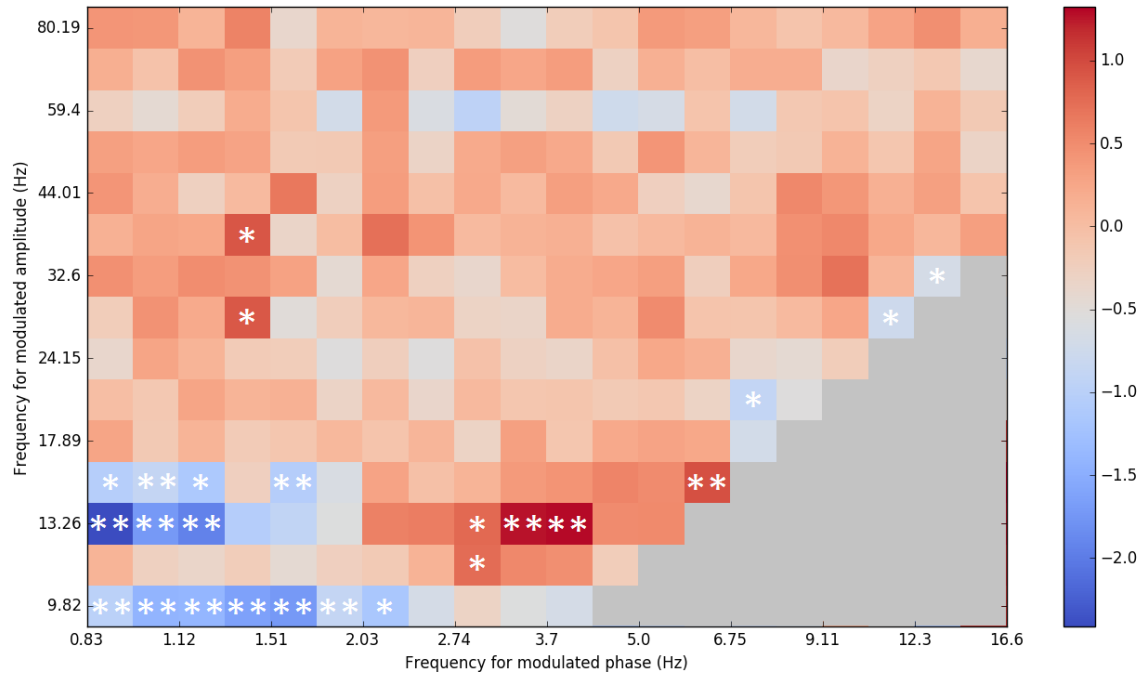


*Figure 21.* Comodulogram for stage differences (N = 10). Colours represent differences (REMS minus NREMS) in normalized log-transformed MIs, averaging between experimental nights. Bandwidths for the amplitude frequency are always double the upper limit of the phase frequency. MI, modulation index. \* $p < 0.05$ , \*\* $p < 0.01$ .